

Using native and synthetic genes to disrupt inositol pyrophosphates and phosphate accumulation in plants

Catherine Freed,¹ Branch Craige,² Janet Donahue,² Caitlin Cridland,² Sarah Phoebe Williams,³ Chris Pereira,² Jiwoo Kim,⁴ Hannah Blice,⁵ James Owen Jr,⁵ Glenda Gillaspay^{1,*}

¹Department of Biochemistry, University of Wisconsin-Madison, Madison, WI 53706, USA

²Department of Biochemistry, Virginia Tech, Blacksburg, VA 24061, USA

³Department of Biology, The College of William & Mary, Williamsburg, VA 23185, USA

⁴Department of BioSciences, Rice University, Houston, TX 77005, USA

⁵Application Technology Research Unit, US Department of Agriculture, Agricultural Research Service, Wooster, OH 44691, USA

*Author for correspondence: glenda.gillaspay@wisc.edu

The author responsible for distribution of materials integral to the findings presented in this article in accordance with the policy described in the Instructions for Authors (<https://academic.oup.com/plphys/pages/General-Instructions>) is: Glenda Gillaspay (glenda.gillaspay@wisc.edu).

Abstract

Inositol pyrophosphates are eukaryotic signaling molecules that have been recently identified as key regulators of plant phosphate sensing and homeostasis. Given the importance of phosphate to current and future agronomic practices, we sought to design plants, which could be used to sequester phosphate, as a step in a phytoremediation strategy. To achieve this, we expressed diadenosine and diphosphoinositol polyphosphate phosphohydrolase (DDP1), a yeast (*Saccharomyces cerevisiae*) enzyme demonstrated to hydrolyze inositol pyrophosphates, in *Arabidopsis thaliana* and pennycress (*Thlaspi arvense*), a spring annual cover crop with emerging importance as a biofuel crop. DDP1 expression in *Arabidopsis* decreased inositol pyrophosphates, activated phosphate starvation response marker genes, and increased phosphate accumulation. These changes corresponded with alterations in plant growth and sensitivity to exogenously applied phosphate. Pennycress plants expressing DDP1 displayed increases in phosphate accumulation, suggesting that these plants could potentially serve to reclaim phosphate from phosphate-polluted soils. We also identified a native *Arabidopsis* gene, Nucleoside diphosphate-linked moiety X 13 (NUDIX13), which we show encodes an enzyme homologous to DDP1 with similar substrate specificity. *Arabidopsis* transgenics overexpressing NUDIX13 had lower inositol pyrophosphate levels and displayed phenotypes similar to DDP1-overexpressing transgenics, while *nudix13-1* mutants had increased levels of inositol pyrophosphates. Taken together, our data demonstrate that DDP1 and NUDIX13 can be used in strategies to regulate plant inositol pyrophosphates and could serve as potential targets for engineering plants to reclaim phosphate from polluted environments.

Introduction

Inorganic phosphate (Pi), a required nutrient for genetic maintenance, cellular function, and energy metabolism, is arguably the greatest plant growth-limiting macronutrient and is indispensable for food production and security on a global scale (Vance et al. 2003). While critically important, Pi is scarce in many agricultural soils and is a rapidly depleting, nonrenewable resource (Cordell et al. 2009). While phosphate deficiency has great global agricultural implications, the overuse of Pi-rich manure and chemical fertilizers to fields often leads to excessive Pi accumulation in soil (Menezes-Blackburn et al. 2018). Moreover, Pi runoff from farmland and urban areas into the watersheds can lead to harmful algal blooms (Gobler 2020). The combination of impending Pi shortages, fertilizer overusage and the negative toxic environmental impacts, described as the Pi crisis, will only become further aggravated with climate change as well as a lack of policy and public awareness (Vaccari 2009; Cordell and White 2011). In the face of these challenges, it is crucial to understand how plants are able to utilize Pi in their environment to develop new solutions to combat the Pi crisis. Under depleted Pi conditions, plants employ molecular mechanisms, collectively known as the Pi starvation response (PSR), to reprioritize growth patterns to increase Pi uptake and redistribute Pi from existing cells (Rouached et al.

2010; Cho et al. 2021; Wang et al. 2021; Madison et al. 2023). The PSR is modulated by complex signaling networks, and while its regulation is not completely understood, emerging evidence strongly supports an integral role for inositol pyrophosphates (PP-InsPs) as central regulators of the PSR (Wild et al. 2016; Dong et al. 2019; Zhu et al. 2019).

PP-InsPs and their precursors, inositol phosphates (InsPs), are important messengers across eukaryotes (Tsui and York 2010; Thota and Bhandari 2015; Azevedo and Saiardi 2017; Shears 2018; Morrisette and Rolfes 2020; Laha et al. 2021). PP-InsPs and InsPs consist of a 6-carbon myo-inositol ring and are sequentially phosphorylated by evolutionarily conserved enzymes (Irvine and Schell 2001; Williams et al. 2015; Livermore et al. 2016; Shears 2018). The number and position of Pi moieties on the ring convey different intracellular messages (Irvine and Schell 2001; Shears 2015; Livermore et al. 2016). InsP₆, also known as phytate when chelated with metals, is the most abundant InsP species found in plants and is important for Pi sensing and storage (Raboy et al. 2001). InsP₆ is implicated as a structural component in plant auxin signaling through binding with the auxin receptor, transport inhibitor 1 (Tan et al. 2007). In plants, InsP₆ can be acted on sequentially by 2 enzymes, the inositol 3,4,5,6-tetrakisphosphate 1-kinase (ITPK), and the diphosphoinositol pentakisphosphate

Received July 22, 2024. Accepted September 28, 2024.

© The Author(s) 2024. Published by Oxford University Press on behalf of American Society of Plant Biologists.

This is an Open Access article distributed under the terms of the Creative Commons Attribution License (<https://creativecommons.org/licenses/by/4.0/>), which permits unrestricted reuse, distribution, and reproduction in any medium, provided the original work is properly cited.

1-kinase (named VIP or VIH), to form the 2 known PP-InsPs, commonly referred to as InsP₇ and InsP₈ (Adepoju et al. 2019; Laha et al. 2019; Whitfield et al. 2020). InsP₇ and InsP₈ are hypothesized to bind and regulate the jasmonate receptor CORONATINE INSENSITIVE1 (COI-1) (Laha et al. 2015, 2016) although InsP₅ has also been implicated due to its presence within the crystallized COI-1 complex (Sheard et al. 2010). Understanding the specific roles of PP-InsPs in these and other plant signaling pathways is an area of emerging interest and requires further examination.

The role of PP-InsPs as critical players in eukaryotic Pi sensing has been facilitated by the examination of loss-of-function mutants in the InsP and PP-InsP synthesis pathways (Dong et al. 2019; Zhu et al. 2019; Land et al. 2021). Specifically, depleting InsP₈ in planta leads to alterations in a plant's ability to properly sense and respond to Pi (Fig. 1) (Dong et al. 2019; Zhu et al. 2019; Land et al. 2021). *Arabidopsis* loss-of-function double mutants for both InsP₈ synthetic enzymes (VIP1 and VIP2, which are also referred to as VIH2 and VIH1, respectively) have depleted levels of PP-InsPs, as well as altered physiological responses to Pi, which include increased Pi accumulation, PSR gene induction, and impacted growth (Dong et al. 2019; Zhu et al. 2019). These data support a model for control of the PSR transcriptional response where InsP₈ controls association of the Phosphate Starvation Response Regulator 1 (PHR1) transcription factor with its binding partner, SPX1 (named after *Saccharomyces cerevisiae* proteins Syg1 and Pho81 and mammalian protein Xpr1; Puga et al. 2014) preventing PHR1-mediated induction of PSR genes (Fig. 1). The SPX domain present within SPX1 has been shown via binding assays to bind InsP₈ at a high affinity (Wild et al. 2016; Ried et al. 2021). A recent study shows that a rice SPX2/InsP₆ (serving as a substitute for InsP₈)/PHR2 complex inhibited the binding of PHR2 to DNA by disrupting PHR2 dimerization (Guan et al. 2022). Taken together, this suggests that InsP₈ can be viewed as a proxy for intracellular Pi levels and is likely the main molecule regulating PHR1-SPX complexes.

It is crucial to understand the extent to which InsPs and PP-InsPs contribute to plant Pi homeostasis and to utilize this information to inform future translational approaches to address the global Pi crisis. While *vih1-2 vih2-4* mutants directly target the enzymes that synthesize InsP₈ (Zhu et al. 2019), the severe growth phenotypes of these mutants make it difficult to explore Pi homeostasis in agronomic conditions. Furthermore, while previous studies focused on plant PP-InsP synthesis enzymes, the enzymes involved in plant PP-InsP degradation are much less characterized. Given this, we have decided to explore the utility PP-InsP phosphatases in impacting plant PP-InsP signaling. Nucleoside diphosphate-linked moiety X (NUDIX) enzymes, along with the phosphatase domain of VIP enzymes (Mulugu et al. 2007; Shears et al. 2017) and SIW14/DSP-PFA enzymes (Aceti et al. 2008; Wang et al. 2018; Gaugler et al. 2022), are the most likely known PP-InsP degrading enzymes that could function to regulate cellular levels of PP-InsPs in plants. The NUDIX clan contains a highly diverse set of phosphohydrolases that are found in all domains of life (Srouji et al. 2017). A total of 27 NUDIX enzymes have been identified in *Arabidopsis* (Kraszewska 2008; Ogawa et al. 2008) and they share a similar, highly conserved NUDIX hydrolase motif similar to diadenosine and diphosphoinositol polyphosphate phosphohydrolase (DDP1) (Sheikh et al. 1998; Xu et al. 2002; Kraszewska 2008). Of these 27 enzymes, only the structures of NUDIX1 (Liu et al. 2018) and NUDIX7 (Tang et al. 2015) have been resolved. Furthermore, the enzymatic activities of about half of these *Arabidopsis* NUDIX enzymes have been empirically explored but the roles of many of the others remain unelucidated

(Kraszewska 2008). Of what has been explored regarding the plant NUDIX enzymes, the role of these enzymes in PP-InsP signaling in plants lacks clarity.

We have focused on developing a synthetic biology approach to directly target and break down PP-InsPs in plants. For this study, we selected DDP1 (gene YOR163w), a phosphatase from *S. cerevisiae* containing a NUDIX hydrolase motif that hydrolyzes phosphoanhydride bonds from PP-InsPs, polyphosphates (polyP; polyP_n), and diadenosine polyphosphates (Ap_nA; specifically, Ap₅A and Ap₆A) (Safrany et al. 1999; Gunawardana et al. 2009; Lonetti et al. 2011; Kilari et al. 2013; Márquez-Moñino et al. 2021). Of these 3 molecule classes, only PP-InsPs have been detected in plants (Desai et al. 2014; Laha et al. 2015) and have a known synthesis pathway (Desai et al. 2014; Laha et al. 2015; Adepoju et al. 2019; Laha et al. 2019). With regard to PP-InsPs, DDP1 has been shown to hydrolyze InsP₈ and InsP₇ isomers, 1-InsP₇ and 5-InsP₇, with the strongest preference for hydrolyzing 1-InsP₇ (Kilari et al. 2013). Here, we report that DDP1 overexpression in *Arabidopsis* decreases PP-InsP accumulation, increases Pi accumulation over the course of plant development, and activates PSR genes. To identify NUDIX enzymes involved in PP-InsP degradation in planta, we have selected NUDIX13 given a protein BLAST using DDP1 as a query identified NUDIX13 as a strong candidate (*e* value of 2e⁻¹⁰) (Altschul et al. 1997; Altschul et al. 2005) as well as its prediction to hydrolyze PP-InsPs (Kraszewska 2008), and its ability to hydrolyze Ap₅A and Ap₆A (Olejnik et al. 2007), which are known DDP1 substrates (Safrany et al. 1999; Lonetti et al. 2011; Kilari et al. 2013; Márquez-Moñino et al. 2021). We hypothesize that NUDIX13 could hydrolyze PP-InsPs and increase plant Pi accumulation. We engineered NUDIX13 gain-of-function transgenics and found that they exhibited similar phenotypes to DDP1 transgenics through Pi toxicity phenotypes, decreased PP-InsPs, and increased Pi accumulation. Herein, we demonstrate that DDP1 and NUDIX13 hydrolyze a group of substrates including InsP₇, InsP₈, Ap₅A, and polyP in vitro and localize to the same subcellular compartments: nucleus and cytosol. Additionally, we explored the translational utility of these changes and transferred the DDP1 gene into a cover crop species, *Thlaspi arvense* (pennycress), and showed that this cover crop model system can increase Pi accumulation from soil. Ultimately, these unique *Arabidopsis* and pennycress transgenics will be useful in understanding the role of PP-InsPs in Pi sensing as well as in informing phytoremediation strategies.

Results

DDP1 overexpression in *Arabidopsis* negatively impacts growth and Pi sensitivity

To reduce PP-InsPs in planta, transgenic lines were generated by overexpressing *S. cerevisiae* DDP1 (YOR163w) (Cartwright and McLennan 1999; Lonetti et al. 2011; Kilari et al. 2013) fused to a C-terminal GFP tag under control of the CaMV 35S promoter in *Arabidopsis* Col-0 plants. DDP1 overexpression lines (DDP1 OX) were confirmed by immunoblotting, which revealed correlation of DDP1-GFP expression with a severe growth phenotype (Fig. 2, A to D). For this study, we selected 3 DDP1 OX lines expressing abundant or very low amounts of DDP1-GFP. DDP1-A and DDP1-I transgenics displayed abundant DDP1-GFP expression and are severely impacted in their growth (Fig. 2, A to D). These plants have a significantly reduced rosette diameter, as well as leaf tip necrosis and leaf chlorosis, phenotypes that are evocative of plant Pi toxicity (Fig. 2, A to C) (Aung et al. 2006; Hu et al. 2011).

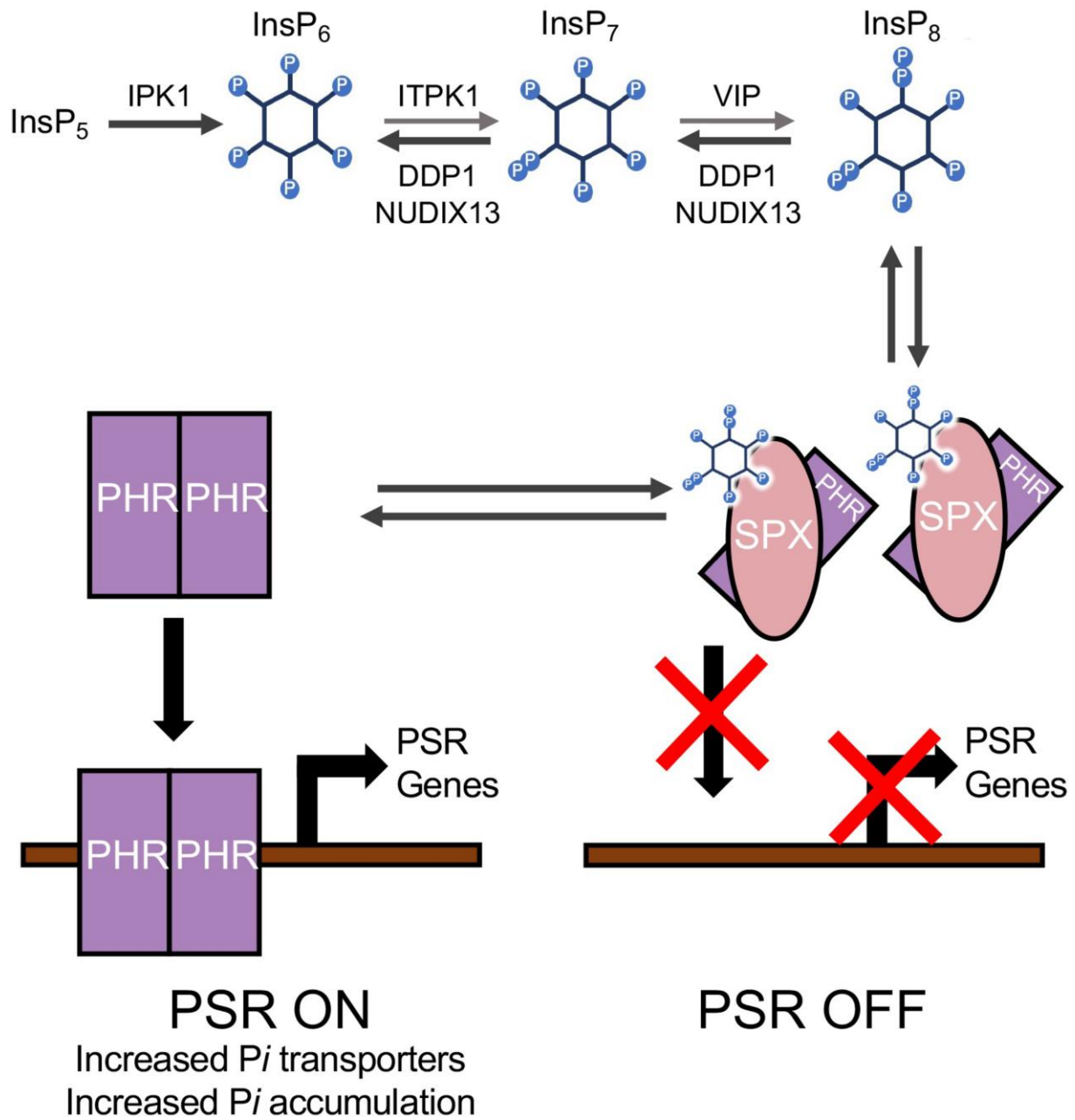


Figure 1. Simplified model for PP-InsP synthesis, degradation, and regulation of PSR genes. IPK1 synthesizes InsP_6 , ITPK enzymes synthesize InsP_7 , and VIP enzymes synthesize InsP_8 in *Arabidopsis*. Transgenic expression of DDP1 (*S. cerevisiae*) or NUDIX13 (*Arabidopsis*) is predicted to hydrolyze InsP_7 and InsP_8 in plants. It is important to note that this is a simplified figure and does not address specific InsP isomers or the newly discovered isomers of InsP_7 (Riemer et al. 2021; Laha et al. 2022). Under Pi-deplete conditions, dimerized PHR binds to the P1BS promoter and upregulates PSR genes ("PSR ON") (Zhou et al. 2021). Under Pi-replete conditions, InsP_8 is assumed to be the controller to turn the PSR off. InsP_8 binds to SPX and this SPX: InsP_8 complex disrupts the PHR dimer and inhibits PHR-mediated transcription of PSR genes.

As DDP1-I and DDP1-A plants begin the reproductive phase, abortion of developing embryos can be seen (Fig. 2B), leading to low recovery of seeds. In contrast, the DDP1-H line has barely detectable levels of DDP1-GFP protein accumulation, does not differ in growth from wild-type (WT) plants, and does not have negatively impacted reproductive phenotypes (Fig. 2, A to D). We compared DDP1 OX lines with a well-characterized PP-InsP-depleted mutant, *ipk1*. *ipk1* harbors a partial loss-of-function mutation in INOSITOL-PENTAKISPHOSPHATE 2-KINASE 1, the only known enzyme in plants to synthesize InsP_6 from InsP_5 (Stevenson-Paulik et al. 2005). *ipk1* mutants are significantly smaller than WT plants, as seen by a reduced rosette diameter, which is a phenotype

observed in previous studies (Stevenson-Paulik et al. 2005; Kuo et al. 2014, 2018). DDP1-I, DDP1-A, and, to a lesser extent, *ipk1* plants exhibit leaf tip necrosis and chlorosis (Fig. 2, A to C), suggesting a sensitivity to Pi.

To test the Pi sensitivity of DDP1 OX plants, we focused on the DDP1-I line and grew plants hydroponically with either $10 \mu\text{M}$ or 1 mM KH_2PO_4 for up to 50 d to simulate Pi-deplete and Pi-replete conditions, respectively. As expected, the growth of WT plants is greatly compromised by Pi-deplete conditions, with a significant reduction in shoot growth (Fig. 2, E and F). In contrast, we found that DDP1 OX transgenics were more comparable in size to WT plants when grown under Pi-deplete conditions though DDP1 OX transgenics

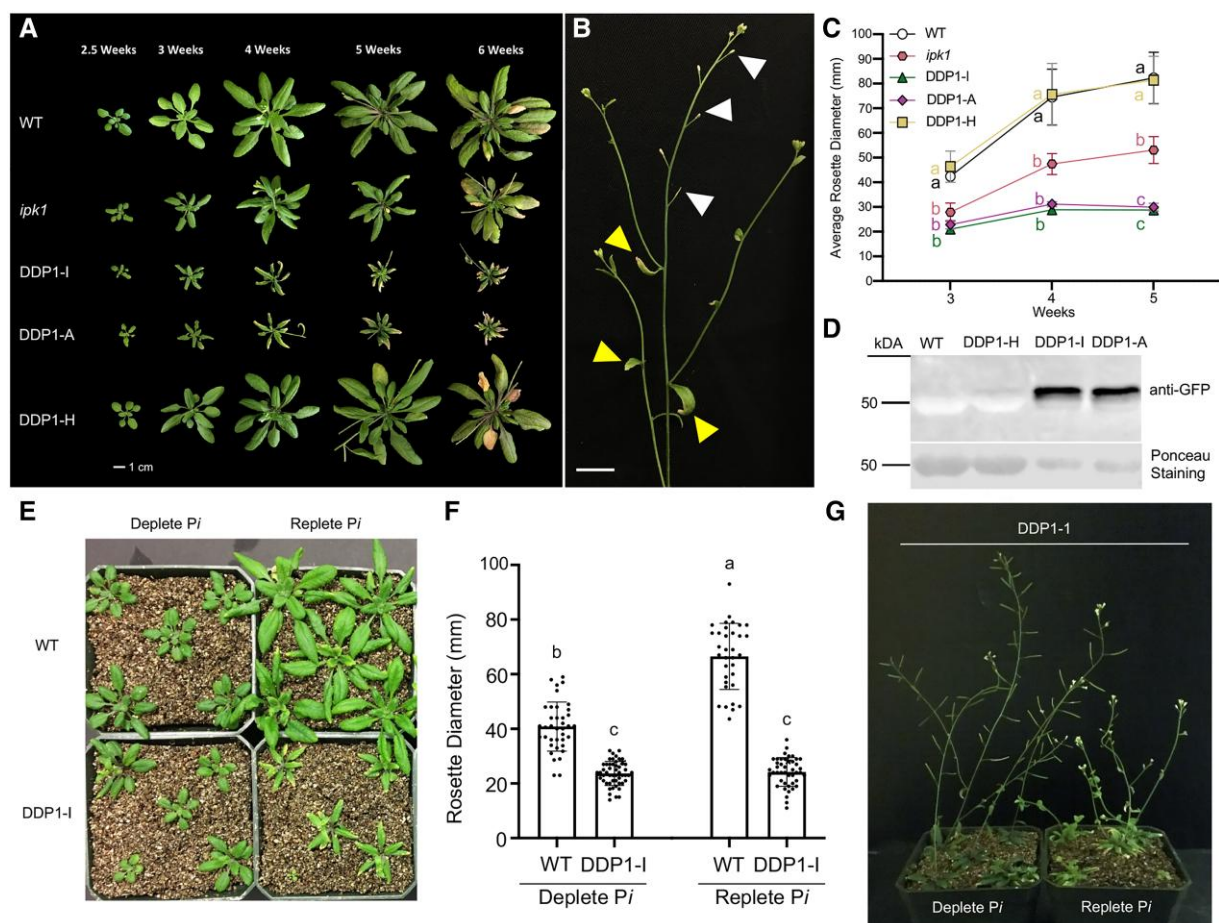


Figure 2. Characterization and comparison of DDP1 OX transgenics. **A)** *Arabidopsis* rosette growth over the course of 6 wk, each image representative of $n = 3$ to 4 independent experiments containing 12 or more plants per genotype. Images were digitally extracted for comparison. Scale bar = 1 cm. **B)** Close-up view of aborting siliques in a 5-wk-old DDP1-I plant. The three white arrowheads at the top of the image indicate aborting siliques, and the three yellow arrowheads at the bottom of the image mark yellowing cauline leaves. Scale bar = 1 cm. **C)** Average rosette diameter over time. Each point represents $n = 3$ independent experiments with over 12 plants per genotype per experiment; error bars show *sd*. Different letters indicate statistically significant means (Tukey honestly significant difference (HSD) test, $\alpha = 0.05$). **D)** Immunoblot of 4-wk-old leaf tissue from WT and selected DDP1 OX transgenics. Ponceau staining shows Rubisco accumulation in all plants as a positive control (~ 50 to 56 kDa). **E)** WT and DDP1 OX transgenics grown on vermiculite containing $0.5\times$ MS media with $10\ \mu\text{M}$ KH_2PO_4 (deplete Pi) or $1\ \text{mM}$ KH_2PO_4 (replete Pi) after 35 d. DDP1-I plants did not accumulate lesions under deplete Pi and resemble WT plants on deplete Pi. **F)** Rosette diameter measurements of WT and DDP1-I grown under deplete and replete Pi. Each point represents an individual plant measurement from $n = 2$ independent experiments; over 35 plants per genotype and condition; error bars show *sd*. Different letters indicate statistically significant means (Tukey HSD, $\alpha = 0.05$). **G)** DDP1-I transgenics after 50 d of growth on vermiculite. DDP1-I lines grown on deplete Pi did not have aborted siliques.

were significantly smaller than WT under both conditions (Fig. 2, E and F). Additionally, while DDP1-I leaves are lighter in color and form brown necrotic lesions in Pi-replete conditions, growth under Pi-deplete conditions results in improvement in growth as seen by a darker leaf color and absence of necrotic lesions (Fig. 2G). A qualitative assessment of seed production indicated that growth of DDP1-I plants under Pi-deplete conditions resulted in a rescue of the embryo abortive phenotype, as seen by DDP1 OX plants with stems and siliques that resembled WT plants after 50 d of growth (Fig. 2G). Leaf and seed phenotypes associated with DDP1 overexpression can be rescued under depleted Pi conditions, indicating that these phenotypes are Pi dependent.

DDP1 overexpression reduces seedling PP-InsP levels

To determine whether DDP1 overexpression alters PP-InsP levels in planta, we measured InsPs and PP-InsPs in all 3 DDP1 OX lines and WT plants using *myo*- ^3H inositol radiolabeling (Desai et al. 2014; Adepoju et al. 2019). We observed a large decrease in InsP₇ and

InsP₈ in DDP1-I and DDP1-A, whereas DDP1-H levels were similar to WT (Fig. 3A; Supplementary Fig. S1A). DDP1-A InsP₇/InsP₆ and InsP₈/InsP₆ ratios were significantly lower than WT ratios (Fig. 3, B and C). DDP1-I also had a significantly lower InsP₈/InsP₆ ratio compared to WT, although the InsP₇/InsP₆ ratio was not statistically significant from WT (Fig. 3B). Interestingly, there was no significant change in the InsP₇/InsP₈ ratio in the severe DDP1 OX lines compared to WT, suggesting that the decrease in InsP₇ and InsP₈ is proportional. Comparing the average percent of InsP₃-InsP₈ species in DDP1 OX transgenic lines to WT (Table 1) showed fluctuations in some InsP species; however, there were no notable changes in any species besides InsP₇ and InsP₈ across all replicates. Of all the InsP species, only InsP₇ and InsP₈ had a consistent decrease in DDP1 OX compared to WT. DDP1-I and DDP1-A, respectively, had $53 \pm 9\%$ and $25 \pm 10\%$ InsP₇ of the total WT InsP₇ pool and $51 \pm 4\%$ and $26 \pm 11\%$ of the total WT InsP₈ pool. Taken together, the data indicate that DDP1 OX lines with higher DDP1-GFP protein accumulation have decreased InsP₇ and InsP₈, which correlates with the observed growth phenotypes of reduced plant size and leaf tip necrosis and chlorosis.

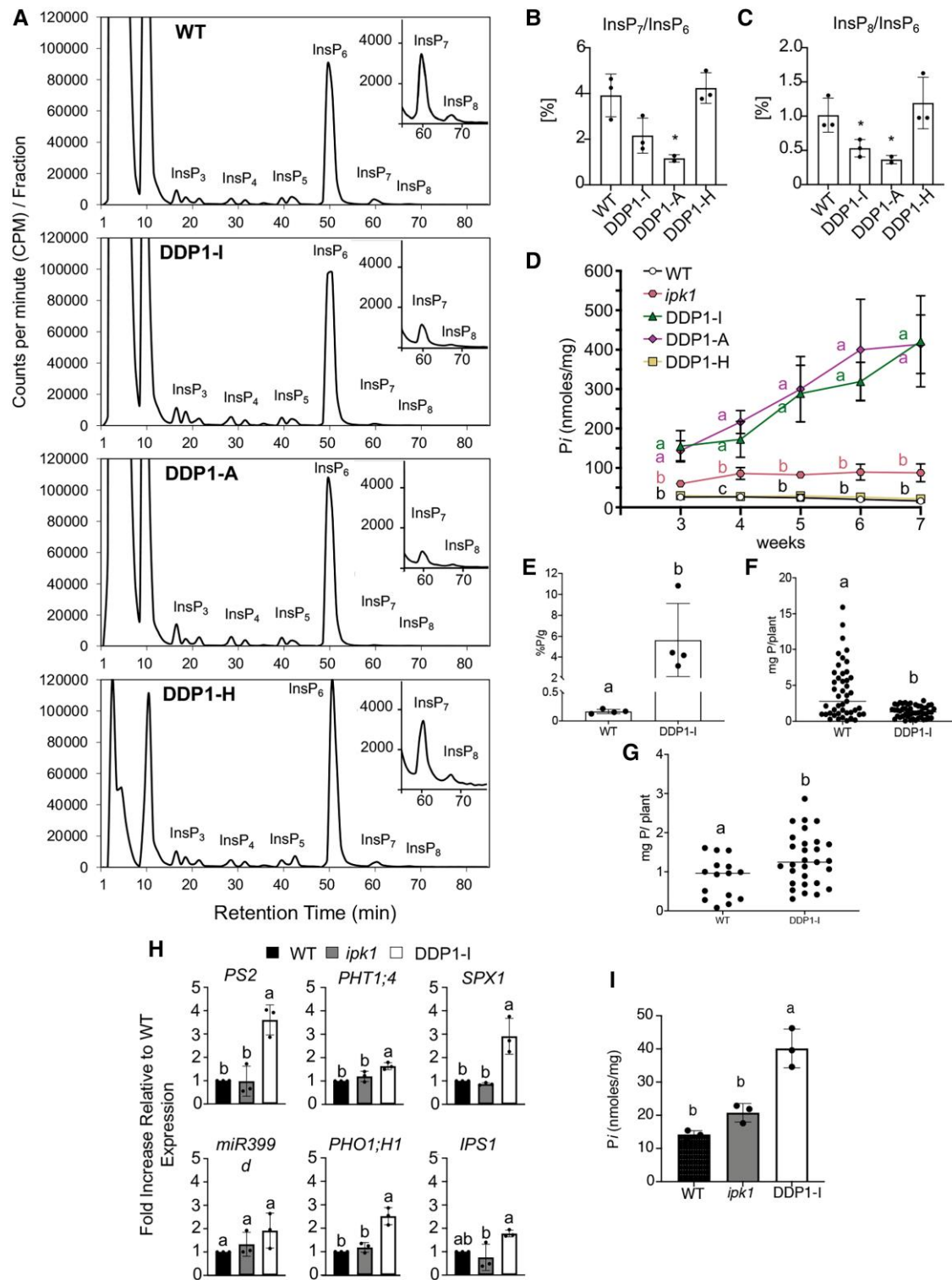


Figure 3. PP-InsP profiling, Pi accumulation, and PSR gene expression in DDP1 OX transgenics. **A)** WT and DDP1 OX transgenics were grown for 14 d on semisolid 0.5× MS media with 0.2% agar then 100 μCi [³H]-myo-inositol was added for 4 d. All InsPs were extracted, separated using anion exchange HPLC, and data were analyzed as described in the “Materials and methods” section. These InsP profiles are representative of 2 to 3 independent replicates per genotype; see [Supplementary Fig. S1](#) for all profiles. **B)** InsP₇/InsP₆ and **C)** InsP₈/InsP₆ ratios. Asterisks show significant differences from WT; analyzed using Student’s t-test; *P < 0.05, error bars show SD of n = 2 to 3. **D)** Leaf Pi accumulation in soil-grown plants from 3 to 7 wk of growth. Each point represents pooled plant tissue from n = 2 to 4 independent experiments; error bars show SD. Different letters indicate statistically significant means (Tukey honestly significant difference (HSD) test, α = 0.05). **E)** Amount of P accumulated in shoot dry mass of WT and DDP1 OX transgenics were grown for 100 d in hydroponic tracks in a greenhouse. **E)** Amount of P accumulated in shoot dry mass of WT and DDP1 OX transgenics. Each point represents the average of one track of n = 9 to 14 plants; error bars show SD (Tukey HSD, α = 0.05). **F)** The amount of total P accumulated per individual plant regardless of total mass (WT n = 45; DDP1 OX n = 49) and **G)** plants weighing 200 mg or less (WT n = 15; DDP1 OX n = 29); (Tukey HSD, α = 0.05). **H)** PSR gene expression (relative to WT) and **I)** Pi accumulation in whole seedlings grown for 10 d grown on media plates. Error bars denote SD of n = 3 independent experiments. Different letters indicate statistically significant means (Tukey HSD, α = 0.05).

Table 1. Average percent of the total counts per minute for each InsP as a percentage compared to the total WT pool for the respective InsP species

	DDP1-H		DDP1-I		DDP1-A	
	Average %	SD	Average %	SD	Average %	SD
InsP ₃	124%	± 42%	129%	± 31%	89%	± 6%
InsP ₄	118%	± 31%	144%	± 29%	157%	± 53%
InsP ₅	99%	± 21%	97%	± 1%	102%	± 46%
InsP ₆	94%	± 19%	102%	± 30%	108%	± 70%
InsP ₇	102%	± 17%	53%	± 9%	25%	± 10%
InsP ₈	122%	± 67%	51%	± 4%	26%	± 11%

Averages are of all replicates shown in Fig. 3A and Supplementary Fig. S1A. Values that represent ~50% or less of the total WT pool are bolded.

DDP1 overexpression impacts Pi accumulation and PSR gene expression

Previous studies show that perturbing PP-InsPs can increase Pi accumulation, which is associated with an upregulation of PSR genes (Kuo et al. 2014, 2018; Laha et al. 2019; Zhu et al. 2019; Land et al. 2021). As DDP1 OX phenotypes are Pi dependent and similar to plants exhibiting symptoms of Pi toxicity, we queried Pi accumulation and expression of a specific set of PSR genes. We first gauged shoot Pi accumulation in soil-grown DDP1 OX transgenics by measuring total shoot Pi accumulation from 3 to 7 wk of growth (Fig. 3D). Both of the severe DDP1 OX lines had an average fold increase of 5.5 to 6 times more Pi compared to WT after 3 wk of growth. Remarkably, Pi accumulation ascended to a 25- to 26-fold increase after 7 wk of growth. This increase in Pi accumulation in DDP1 OX was also significantly higher than what we observed in *ipk1* mutants (Fig. 3D). This is notable as *ipk1* mutants accumulated significantly higher Pi compared to WT both in our experiments and in previous studies (Kuo et al. 2014, 2018; Land et al. 2021). DDP1-H transgenics showed no difference in Pi accumulation compared to WT plants (Fig. 3D). Most strikingly, a comparison of *ipk1* and severe DDP1 OX line patterns of Pi accumulation over time indicates that whereas Pi accumulation in *ipk1* plants reaches a maximum at 3 wk, DDP1 OX plants continue to accumulate significantly elevated levels of Pi over time. Given the differences in WT and DDP1 OX size, we were curious to know how much total phosphorus (P) was being absorbed by the plants. We queried the total P accumulation capacity of 100-d-old WT and DDP1-I plants grown under hydroponic conditions and reported that DDP1-I shoot tissue accumulated a significantly higher enrichment of P per gram compared to WT shoots (Fig. 3E). We also quantified the total P absorption on an individual plant basis. Overall, WT plants accumulated significantly higher levels of P on an individual plant basis compared to DDP1-I OX plants (Fig. 3F). Notably, WT plants of similar size to DDP1-I OX plants at the time of harvest (200 mg or less) showed significantly lower levels of P accumulation compared to DDP1-I OX transgenics. Taken together, these data suggest that while the current growth tradeoff of DDP1-I OX is not ideal for P absorption compared to WT plants with a larger mass, overexpression of DDP1 in *Arabidopsis* leads to a higher enrichment of P in the plant.

Given the increase in Pi accumulation, we hypothesized that these increases were linked to increased expression of PSR genes. We queried a subset of PSR marker genes that play key roles in plant Pi accumulation under Pi-deplete conditions (SPX1, PS2, *miR399d*, *PHT1;4*, *PHO1;H1*, and *IPS1*) (Rouached et al. 2010; Jost et al. 2015; Chien et al. 2018). Of the genes queried, we observed

that 10-d-old DDP1 OX whole seedlings showed a significant upregulation of PS2, *PHT1;4*, *SPX1*, and *PHO1;H1* compared to WT and *ipk1* seedlings (Fig. 3H). DDP1-I also had significantly increased *IPS1* compared to *ipk1*; however, this change was not significantly different from WT. *ipk1* seedlings trended toward increased expression of a few genes within the queried subset; however, these changes were not statistically significant. This result was expected as *ipk1* whole seedlings have not been shown to induce the PSR under replete conditions (Zhu et al. 2019), although it is important to consider that previous studies querying PSR gene expression specifically in *ipk1* roots show significant increases in PSR gene expression (Kuo et al. 2014, 2018). Pi accumulation in these 10-d-old seedlings was also queried, and we found, as expected, that DDP1-I plants accumulated significantly more Pi compared to WT and *ipk1* (Fig. 3I).

NUDIX13 overexpression decreases PP-InsPs and increases Pi accumulation

We sought to determine if similar PP-InsP reductions and Pi accumulation patterns could be achieved by overexpressing the native *Arabidopsis* enzyme, NUDIX13, given this enzyme shares predicted (Kraszewska 2008) and known substrates (Olejnik et al. 2007) with DDP1. Using the same strategy that we used for our stable DDP1 OX transgenics, NUDIX13-GFP transgenic plants were generated in the *Arabidopsis* Col-0 background with the CaMV 35S promoter. Two lines (NUDIX13-H and NUDIX13-O) were found to have high accumulation of NUDIX13-GFP (Fig. 4A) and were prioritized for our study. Similar to, yet less severe than the DDP1 OX transgenics, NUDIX13 OX plants had significantly smaller rosettes and exhibited leaf tip necrosis and chlorosis phenotypes (Fig. 4, B to D). NUDIX13-H and NUDIX13-O showed no significant difference from *ipk1* plants in terms of rosette diameter size but appeared to have larger zones of leaf tip necrosis and chlorosis on rosette and cauline leaves compared to *ipk1* (Fig. 4, C and D).

Quantification of PP-InsPs in NUDIX13-O and NUDIX13-H plants revealed significant decreases in InsP₇ and InsP₈ pools compared to WT plants (Fig. 4, E to G; Supplementary Fig. S2). NUDIX13-O and NUDIX13-H had significantly lower InsP₇/InsP₆ ratios compared to WT (Fig. 4H). InsP₈/InsP₆ ratios trended to be lower than WT but were not significant (Fig. 4I), and NUDIX13-O had significantly higher InsP₈/InsP₇ ratios compared to WT whereas NUDIX13-H trended to be higher but was not significant (Supplementary Fig. S2B). Based on these ratios and quantification of InsP species as compared to WT pools, the decrease in InsP₇ and InsP₈ appeared to be proportional in NUDIX13 transgenics (Fig. 4, F and G; Table 2). Comparing the average percent of InsP₃-InsP₈ species in all lines compared to WT revealed that there were no significant changes in any InsP species except for InsP₇ and InsP₈ (Table 2). NUDIX13-O and NUDIX13-H, respectively, displayed 35 ± 4% and 36 ± 0% InsP₇ of the total WT InsP₇ pool, and 48 ± 4% and 39 ± 2% of the total WT InsP₈ pool.

We also quantified PP-InsP accumulation in a loss-of-function *Arabidopsis* mutant carrying a T-DNA insertion in NUDIX13, designated here as *nudix13-1* (SALK_031617). In contrast to the reduction in InsP₇ and InsP₈ seen in NUDIX13 OX transgenics, *nudix13-1* mutants accumulated significantly higher levels of InsP₇ and InsP₈ as compared to WT plants (Supplementary Fig. S3; Table 2). *nudix13-1* mutants contained 207% ± 5% InsP₇ and 128% ± 15% InsP₈ of the WT PP-InsP pools (Table 2). Additionally, *nudix13-1* contained significantly higher levels of InsP₄ and InsP₅ and lower levels of InsP₆ as compared to WT plants

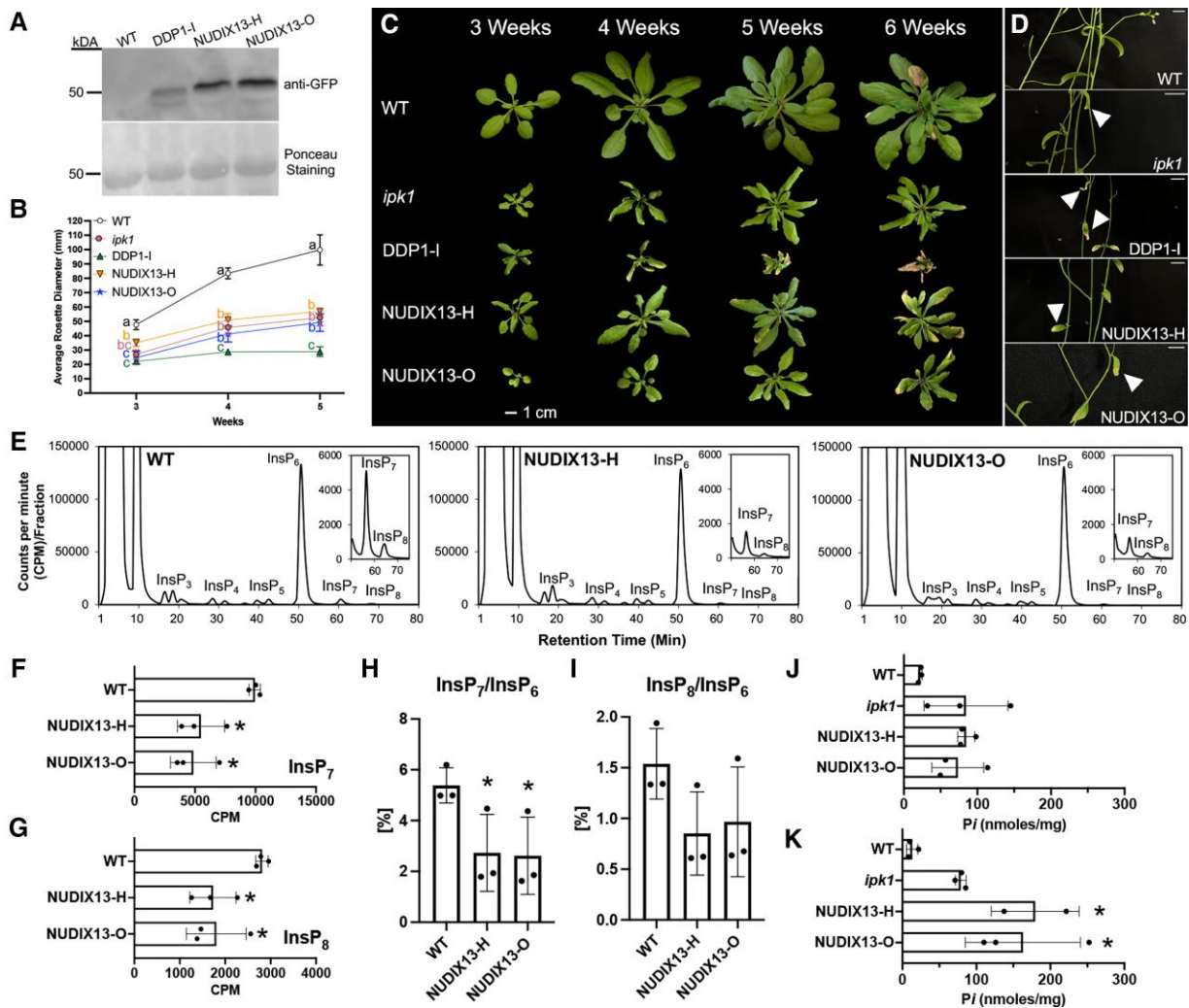


Figure 4. Characterization of NUDIX13 OX transgenics. **A)** Immunoblot of 3-wk-old leaf tissue from WT and selected NUDIX13 OX transgenics. Ponceau staining shows Rubisco accumulation in all plants as a positive control (~50 to 56 kDa). **B)** Average rosette diameter over time. Each point represents $n = 3$ independent experiments with over 12 plants per genotype per experiment; error bars show SD . Different letters indicate statistically significant means (Tukey honestly significant difference (HSD) test, $\alpha = 0.05$). **C)** *Arabidopsis* rosette growth over the course of 5 wk, each image representative of $n = 4$ to 5 independent experiments containing 12 or more plants per genotype. Images were digitally extracted for comparison. Scale bar = 1 cm. **D)** Close-up view of yellowing cauline leaves. White arrowheads indicate yellowing cauline leaves. Scale bar = 1 cm. **E)** HPLC analysis of WT and NUDIX13 OX transgenics, $n = 3$. See [Supplementary Fig. S2](#) for additional profiles. **F)** Total $InsP_7$, **G)** total $InsP_8$, **H)** $InsP_7/InsP_6$, and **I)** $InsP_8/InsP_6$ ratios for additional profiles. Asterisks show significant differences from WT; analyzed using Student's t-test; $*P < 0.05$, error bars show SD of $n = 3$. **J, K)** Leaf Pi accumulation in soil-grown plants from 3 **J)** and 6 wk **K)** of growth. Analyzed using Student's t-test; $n = 2$ to 3 independent experiments; $*P < 0.05$, error bars show SD .

Table 2. The average percent of total, individual $InsP$ species compared to the total WT pool expressed as a percentage. Averages for NUDIX13 OX were taken from all replicates shown in [Fig. 4](#) and [Supplementary Fig. 2](#) and *nudix13-1* from [Supplementary Fig. S3](#); $n = 3$ biological replicates per genotype

	NUDIX13-O		NUDIX13-H		<i>nudix13-1</i>	
	Average %	SD	Average %	SD	Average %	SD
$InsP_3$	91%	$\pm 2\%$	109%	$\pm 8\%$	96%	$\pm 4\%$
$InsP_4$	96%	$\pm 4\%$	105%	$\pm 13\%$	<u>127%</u>	<u>$\pm 4\%$</u>
$InsP_5$	92%	$\pm 0\%$	102%	$\pm 9\%$	<u>139%</u>	<u>$\pm 1\%$</u>
$InsP_6$	105%	$\pm 3\%$	100%	$\pm 3\%$	89%	$\pm 1\%$
$InsP_7$	35%	$\pm 4\%$	36%	$\pm 0\%$	<u>207%</u>	<u>$\pm 5\%$</u>
$InsP_8$	48%	$\pm 4\%$	39%	$\pm 2\%$	<u>128%</u>	<u>$\pm 15\%$</u>

Values that represent ~50% or less of the total WT pool are bolded. Values that represent ~120% or higher of the total WT pool are underlined.

([Supplementary Fig. S3](#); [Table 2](#)). This demonstrates that disruption of NUDIX13 alters plant $InsP$ and PP- $InsP$ profiles in a way consistent with a native function in hydrolyzing PP- $InsPs$.

Given decreased plant growth and decreased PP- $InsP$ accumulation, we also measured Pi accumulation in NUDIX13 OX shoot tissue. NUDIX13 OX lines had accumulated significantly higher levels of Pi compared to WT after 3 and 6 wk of growth ([Fig. 4, J and K](#)). We report that there was no significant difference in Pi accumulation in NUDIX13 OX lines compared to WT or *ipk1* mutants after 3 wk of growth ([Fig. 4J](#)). After 6 wk of growth, NUDIX13 OX lines accumulated significantly higher levels of Pi compared to WT plants ([Fig. 4K](#)). Taken together, our data demonstrate that DDP1 OX and NUDIX13 OX lines are similarly impacted through decreased plant size, Pi toxicity phenotypes, decreased PP- $InsPs$, and increased Pi accumulation.

NUDIX13 hydrolyzes PP- $InsPs$ and other predicted substrates in vitro

While our in planta data are indicative of NUDIX13 breaking down PP- $InsPs$, we sought to confirm this through in vitro phosphatase assays. We purified recombinant DDP1-GST, NUDIX13-GST, and

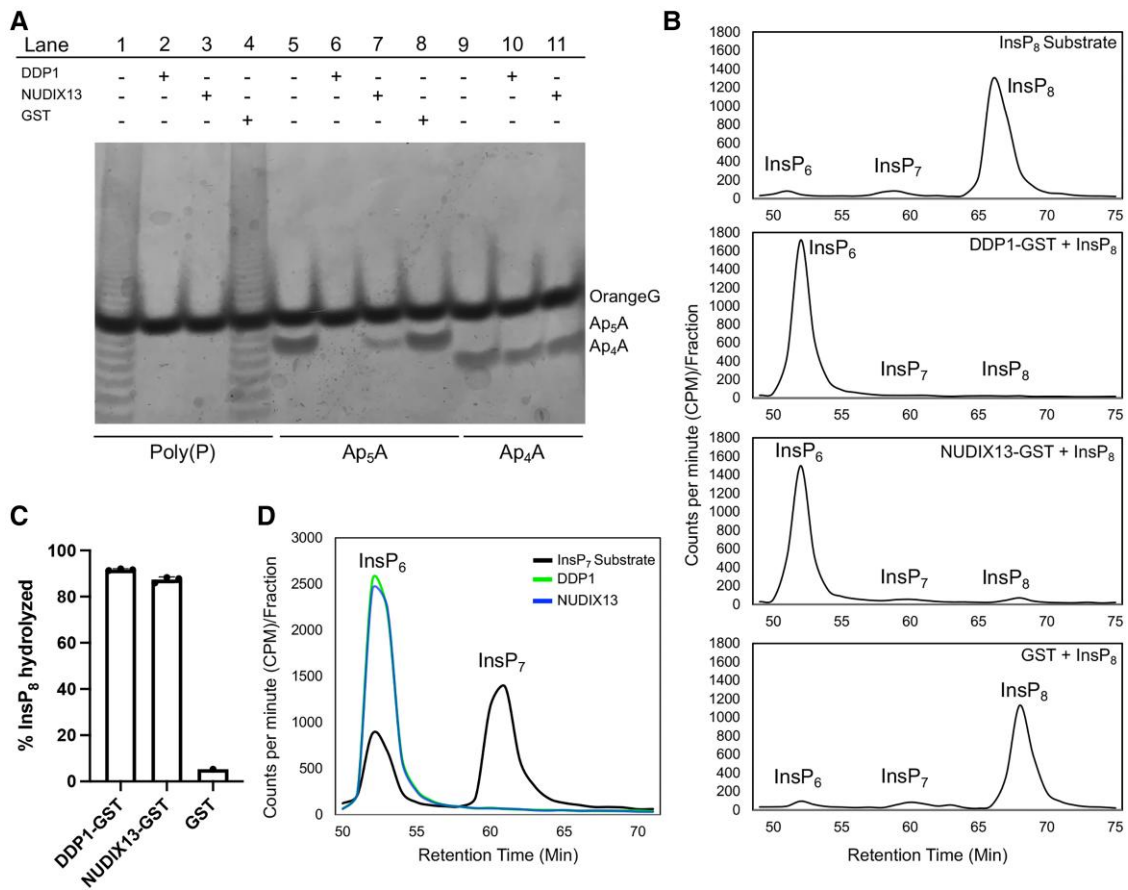


Figure 5. In vitro phosphatase assays with purified recombinant DDP1-GST and NUDIX13-GST. **A)** Purified DDP1-GST, NUDIX13-GST, or GST alone (negative control) was incubated with polyP (Lanes 1 to 4), Ap₅A (Lanes 5 to 8), or Ap₄A (Lanes 9 to 11) for 1.5 h at 37 °C, and then the reactions were resolved by PAGE and stained with Toluidine blue. Bands corresponding to Orange G (loading dye), Ap₅A, and Ap₄A are indicated on the right; undigested polyP appears ladderlike. Reactions in the absence (–) or presence (+) of enzyme or control GST protein are indicated in the table. **B to D)** DDP1-GST, NUDIX13-GST, or GST alone (negative control) was incubated with radiolabeled InsP₈ **B)** or InsP₇ **D)** for 1.5 h at 37 °C, and then the reaction products were resolved by HPLC and measured by liquid scintillation counting. Representative chromatograms with peaks corresponding to InsP₆, InsP₇, or InsP₈ are shown. Reactions that lacked enzyme or GST control protein (traces labeled “InsP_{7/8} substrate”) show the starting substrate in each reaction. **C)** Percentage of InsP₈ hydrolyzed by each enzyme (*n* = 3); error bars show SD. **D)** HPLC analyses of enzymatically synthesized InsP₇ substrate incubated with DDP1 or NUDIX13, or without enzyme, *n* = 1.

GST (Olejnik et al. 2007; Ogawa et al. 2008; Márquez-Moñino et al. 2021) for our assays. GST was used as a negative control for substrate degradation. To ensure the purified enzymes were active, we used Ap₅A as a positive control for hydrolysis and Ap₄A as a negative control (Olejnik et al. 2007; Ogawa et al. 2008; Lonetti et al. 2011; Andreeva et al. 2019). We also included polyP as a substrate since DDP1 has been empirically shown to break down polyP in vitro (Lonetti et al. 2011; Andreeva et al. 2019). Our data indicate that purified DDP1-GST and NUDIX13-GST are active as shown through hydrolysis of Ap₅A and polyP (Fig. 5A). Neither enzyme hydrolyzed Ap₄A, which is consistent with previous reports. NUDIX13 is also capable of hydrolyzing polyP, indicating its similarity in substrate preferences as DDP1. To compare to our in planta PP-InsP data, InsP₇ and InsP₈ molecules were enzymatically synthesized, as previously described in Adepoju et al. (2019). DDP1-GST, NUDIX13-GST, and GST were then incubated with InsP₇ and InsP₈ for 1.5 h, separated using HPLC, and detected by scintillation counting (Desai et al. 2014; Adepoju et al. 2019). Our data demonstrate that DDP1 and NUDIX13 hydrolyze InsP₇ and InsP₈ in vitro, with roughly 90% InsP₈ hydrolyzed after a 1.5-h incubation (Fig. 5, B and C). DDP1 and NUDIX13 also hydrolyzed InsP₇ when incubated with an enzymatically synthesized InsP₇

substrate (Fig. 5D). Collectively, our data demonstrate that DDP1 and NUDIX13 hydrolyze PP-InsPs, Ap₅A, and polyP in vitro.

DDP1-GFP and NUDIX13-GFP colocalize with PP-InsP synthetic enzymes

Since DDP1 and NUDIX13 hydrolyze PP-InsPs in vitro and in planta, we sought to determine if the subcellular localization of DDP1 and NUDIX13 in planta was similar to the enzymes that synthesize PP-InsPs. While the native locations of PP-InsPs have yet to be determined in vivo, many of the PP-InsP synthesis enzymes in plants localize to the cytoplasm and nuclei (Xia et al. 2003; Kuo et al. 2018; Adepoju et al. 2019). Subcellular distribution of DDP1-GFP and NUDIX13-GFP under control of the CaMV 35S promoter was assessed using confocal microscopy in transgenic *Arabidopsis* lines and infiltrated *Nicotiana benthamiana* leaves. Both constructs localized predominantly to the cytoplasm and nuclei of *Arabidopsis* cells (Fig. 6, A to L). Consistent with our immunoblotting data, GFP signal was abundant in DDP1-I, DDP1-A, NUDIX13-H, and NUDIX13-O cells and undetectable in WT and DDP1-H (Fig. 6, A to F; Supplementary Fig. S4). GFP expression was also high in guard cell nuclei (Fig. 6B). We transiently

coexpressed DDP1-GFP or NUDIX13-GFP in *N. benthamiana* with 2 plant organelle marker constructs: unconjugated mCherry, which localizes to the cytoplasm and nucleus (Adepoju et al. 2019), and endoplasmic reticulum (ER)-mCherry, a construct that localizes to the ER (Nelson et al. 2007). We also included YFP-DDP1 (DDP1 with an N-terminal YFP tag) to increase confidence that the localization pattern was not influenced by the position of the tag. DDP1-GFP, NUDIX13-GFP, and YFP-DDP1 colocalize substantially with unconjugated mCherry in the nucleus and the cytoplasm (Fig. 6, G to L). In contrast, we observed little if any colocalization with the ER-mCherry marker (Supplementary Figs. S5 to S7). YFP-DDP1 localized to the same compartments as DDP1-GFP, confirming that the pattern was not impacted by the position of the tag (Supplementary Fig. S7). Taken together, our data show that DDP1 and NUDIX13 both localize to the cytoplasm and nucleus in compartments, which is consistent with that of other PP-InsP synthesis enzymes.

DDP1 overexpression in pennycress recapitulates *Arabidopsis* phenotypes

Based on the unique ability of DDP1 OX and NUDIX13 OX plants to accumulate higher amounts of Pi over time, we sought to translate this into a strategy to develop a cover crop to recover excess Pi from soil. For this study, we focused on DDP1 given its increased capacity for Pi accumulation compared to NUDIX13 OX transgenics. We selected *T. arvense* (pennycress), a winter annual cover crop that is commonly used by farmers and shows promise as a biofuel crop (Chopra et al. 2020). Notably, recent strides have been made to establish pennycress as a model cover crop system through its recently sequenced genome and assembled transcriptome, and like *Arabidopsis*, it can be easily transformed by floral dipping (McCormick 2018), making it an ideal system for translation of our findings in *Arabidopsis*. We demonstrated that pennycress plants can be stably transformed to overexpress DDP1 and show similar phenotypes as *Arabidopsis* DDP1 OX transgenics (Fig. 7). It is important to note that we characterized heterozygotes in this study as our homozygous pennycress lines were severely growth compromised and displayed extreme Pi toxicity (Supplementary Fig. S8). After 5 wk of growth, the DDP1-B OX line with higher transgenic protein accumulation manifested leaf tip necrosis and chlorosis phenotypes similar to what we observed in *Arabidopsis* (Fig. 7, A to C). Our pennycress DDP1 OX transgenics overexpress DDP1 with an N-terminal YFP tag, which accumulates in the same subcellular compartments (nuclear and cytosolic) as in *Arabidopsis* DDP1 OX plants and *N. benthamiana* leaf tissue (Fig. 7D). Strikingly, pennycress DDP1-B OX plants exhibit significantly higher Pi accumulation compared to WT and the WT-like DDP1-L OX line that expresses undetectable levels of YFP-DDP1 (Fig. 7E). Taken together, these data demonstrate that overexpression of DDP1 in pennycress recapitulates many of the same phenotypes that we observed in *Arabidopsis*, including DDP1 subcellular localization, Pi toxicity phenotypes, and increased Pi accumulation in leaf tissue.

Discussion

The identification of PP-InsP signaling components in plants, along with compelling evidence connecting PP-InsPs to Pi sensing (Laha et al. 2015; Kuo et al. 2018; Adepoju et al. 2019; Laha et al. 2019; Zhu et al. 2019; Land et al. 2021; Laha et al. 2022) has yielded valuable genetic targets for Pi phytoremediation approaches. Manipulation of the PP-InsP signaling pathway in plants offers

an opportunity to address the Pi crisis. In this work, we sought to use a synthetic biology approach to manipulate PP-InsPs in transgenic plants to facilitate the study of the long-term consequences of decreasing PP-InsPs on Pi accumulation and to evaluate the preliminary translational potential of depleting PP-InsPs to increase Pi accumulation in planta. While previous work explores the impact of VIP (Mulugu et al. 2007; Shears et al. 2017) and SIW14/DSP-PFA (Aceti et al. 2008; Wang et al. 2018; Gaugler et al. 2022) plant enzymes, we explored the role of 2 NUDIX enzymes and their impact on plant PP-InsP hydrolysis.

Expression of a synthetic gene, DDP1, and a native gene, NUDIX13, allows plants to accumulate large amounts of Pi

DDP1 OX transgenics with higher DDP1 protein accumulation created growth-compromised plants with Pi toxicity phenotypes and negatively impacted reproductive phenotypes (Figs. 2 and 7). These distinct DDP1 OX phenotypes are Pi dependent as growing DDP1 OX transgenics on depleted Pi conditions rescued the leaf and seed phenotypes (Fig. 2, E to G). Notably, DDP1 OX overexpression decreases PP-InsPs (Fig. 3, A to C), increases PSR gene expression (Fig. 3H), and confers a unique Pi-accumulating phenotype (Figs. 3, D to E, and 7E) with promising translational applications. To explore native plant PP-InsP phosphatases, we identified *Arabidopsis* NUDIX13 as an ideal enzyme given its similarities to DDP1 in structural homology (Olejnik et al. 2007) and predicted function (Kraszewska 2008). Our in vitro experiments demonstrate that recombinant DDP1 and NUDIX13 hydrolyze PP-InsPs, polyP, and Ap₅A (Fig. 5). These results align with previous studies that assessed substrate hydrolysis of DDP1 (Safrany et al. 1999; Lonetti et al. 2011; Andreeva et al. 2019; Márquez-Moñino et al. 2021) and NUDIX13 (Olejnik et al. 2007; Ogawa et al. 2008).

Our data show that stable NUDIX13 expression in *Arabidopsis* is similar to DDP1 OX transgenics, as NUDIX13 OX transgenics were also smaller in size and displayed Pi toxicity phenotypes (Fig. 4). Transgenics expressing high levels of DDP1 and NUDIX13 exhibited decreased PP-InsPs with a similar trend in proportionally reduced InsP₇ and InsP₈ levels (Figs. 3, A and B, and 4, E to I); however, NUDIX13 OX plants were less growth compromised compared to DDP1 OX plants (Fig. 4, B and C). Moreover, while NUDIX13 OX shoot tissue accumulated lower levels of Pi compared to DDP1 OX plants, NUDIX13 OX plants had significantly higher levels of Pi accumulation than WT after 6 wk of growth (Fig. 4K). Taken together, these data suggest that both DDP1 and NUDIX13 are similar enzymes that, when overexpressed in planta, can reduce PP-InsPs and increase plant Pi accumulation.

Overexpression of PP-InsP phosphatases results in unique biological characteristics distinct from PP-InsP kinase mutants

DDP1 and NUDIX13 overexpression in planta allowed us to achieve our original goal of reducing PP-InsPs. This strategy is unique from studying InsP and PP-InsP synthesis mutants. There are 3 types of InsP or PP-InsP synthesis mutants with defects in Pi sensing that have been described in the current literature; the functions of the WT-encoded enzyme products of these mutants are shown in Fig. 1. *ipk1* mutants have reduced levels of PP-InsPs as IPK1 enzyme synthesizes PP-InsP precursor, InsP₆ (Laha et al. 2015; Kuo et al. 2018; Land et al. 2021). Similarly, *itpk1* mutants also showed a reduction in InsP₇ (Kuo et al. 2018) and InsP₈ (Laha et al. 2022) compared to WT seedlings. *vih1-2vih2-4* double mutants were reported to have undetectable levels of InsP₈ and

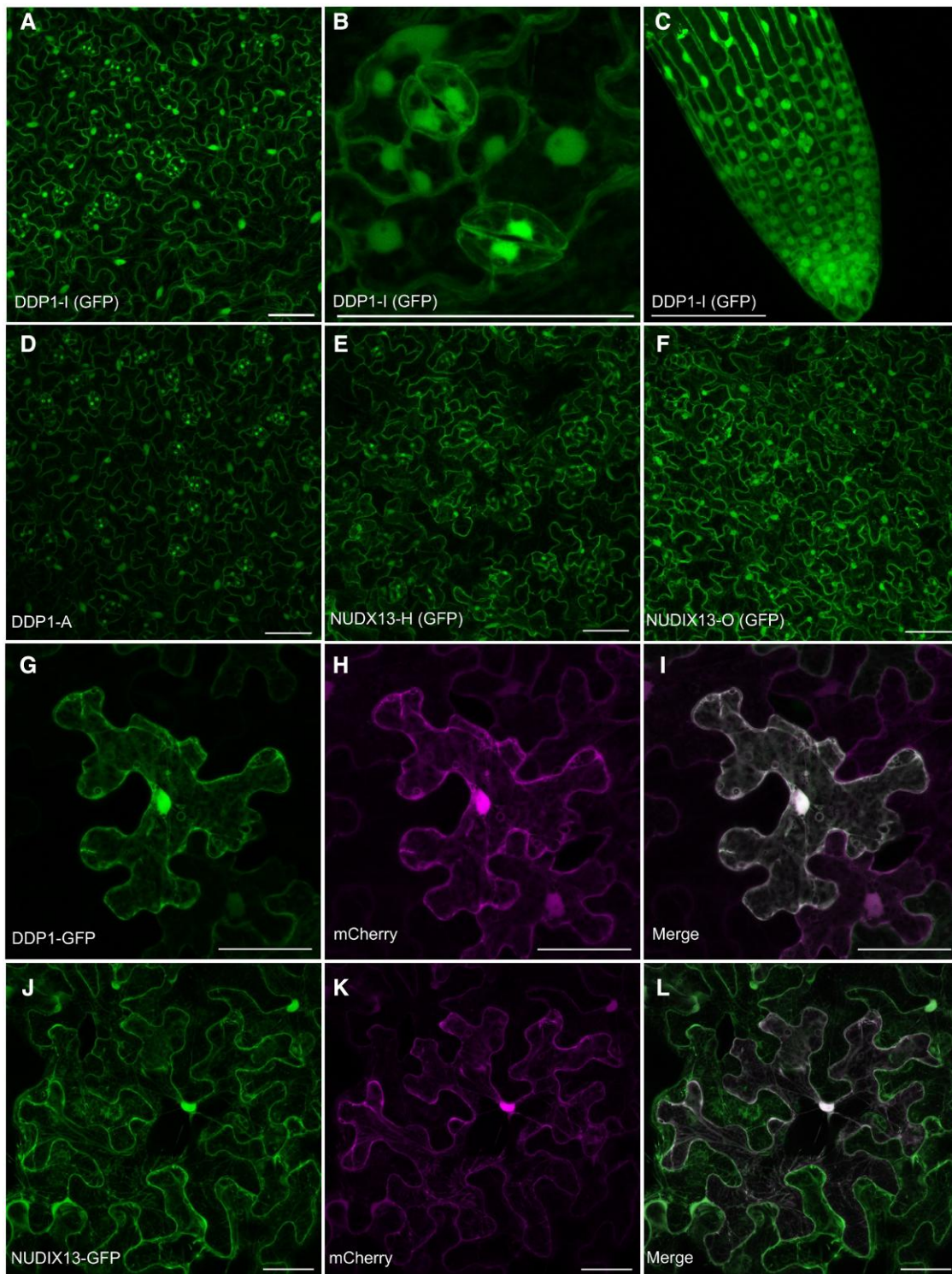


Figure 6. Confocal imaging of DDP1-GFP and NUDIX13-GFP expression in *Arabidopsis* and *N. benthamiana*. **A, B)** *Arabidopsis* DDP1-I leaves and **C)** roots, **D)** DDP1-A leaves, **E)** NUDIX13-H leaves, and **F)** NUDIX13-O leaves. **G)** CaMV35S:DDP1-GFP and **J)** CaMV35S:NUDIX13-GFP transient expression in *N. benthamiana* leaves 48-h postinfiltration. *N. benthamiana* leaves coinfiltrated with DDP1-GFP **G** to **I)** or NUDIX13-GFP **J** to **L)** with unconjugated mCherry. DDP1-GFP and NUDIX13 are shown in green, and unconjugated mCherry is shown in magenta. All images are presented as maximum intensity projections from confocal Z-stack optical sections. All scale bars = 50 μm .

double the WT pool of InsP_7 , in addition to a loss in viability (Zhu et al. 2019). All characterized mutants showed Pi-dependent growth phenotypes, increases in shoot Pi accumulation compared to WT plants, and an induction of PSR genes (Kuo et al. 2014, 2018; Zhu et al. 2019). This induction of the PSR is thought to result from

the lack of InsP_8 available within these mutants, which acts to release the PHR1 transcription factor.

While there are similarities in the way that PP- InsPs levels are altered in previously characterized PP- InsP synthetic mutants and the plants described in our work, there are key differences

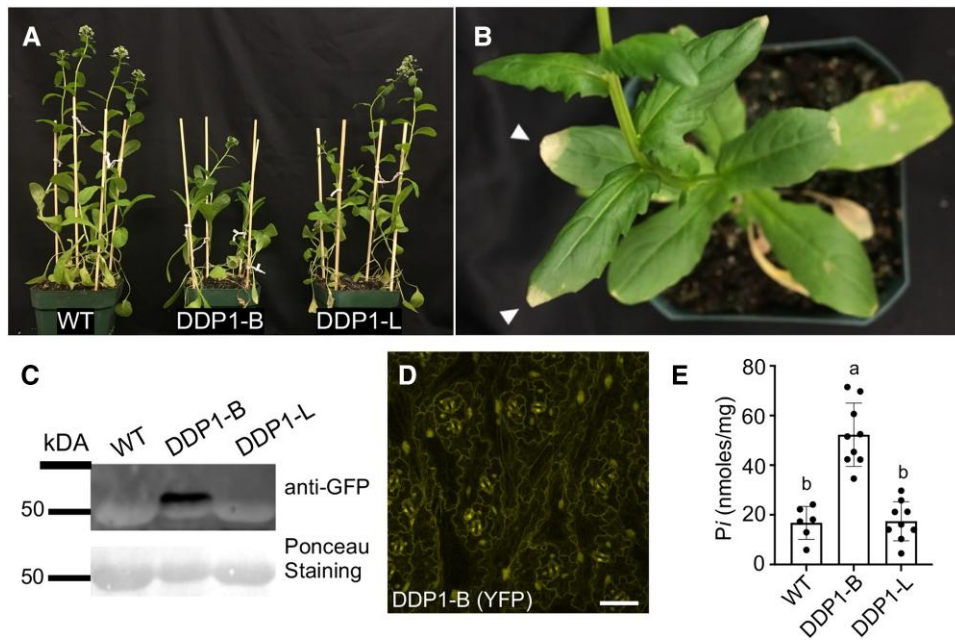


Figure 7. Characterization of pennycress DDP1 OX transgenics. **A)** Physiology of WT pennycress and 2 independent heterozygous DDP1 OX transgenics after 5 wk of growth. **B)** Close-up view of DDP1-B leaf tip necrosis and chlorosis after 7 wk of growth on soil. White arrowheads mark yellowing of leaf tips. **C)** Immunoblot of 6-wk-old leaf tissue from WT and heterozygous pennycress DDP1 OX lines. Ponceau staining shows Rubisco accumulation in all plants as a positive control (~50 to 56 kDa). **D)** Stable YFP-DDP1 expression in pennycress DDP1-B leaves. Scale bar = 50 μ m. **E)** Shoot Pi accumulation in 6- to 7-wk-old pennycress leaf tissue. Error bars denote SD of $n = 3$ independent experiments; each point represents leaf tissue of an individual heterozygous plant. Different letters indicate statistically significant means (Tukey honestly significant difference (HSD) test, $\alpha = 0.05$).

worth noting. First, DDP1 and NUDIX13 OX transgenics actively hydrolyze PP-InsPs in contrast to loss-of-function mutants that lack enzymes that synthesize InsP₆ and/or PP-InsPs. We hypothesize that DDP1 and NUDIX13 in our transgenics are able to hydrolyze InsP₇ and InsP₈ faster than the PP-InsP synthesis enzymes are able to replenish PP-InsP pools (Fig. 1). This hypothesis draws from suggestions over the years that PP-InsP turnover is a cyclical interconversion between InsP₆, InsP₇ isomers, and InsP₈ based on current evidence in yeast and humans (Kilari et al. 2013; Shears 2018; Dollins et al. 2020). Thus, we have likely tipped the delicate scale of this continual cycle of PP-InsP degradation and synthesis by increasing the phosphatases in the mix. Another key difference between our DDP1 OX plants and *ipk1* mutants is the level and duration of Pi accumulation (Fig. 3D). While our work and that of others show that *ipk1* mutants tend to accumulate higher Pi compared to WT plants (Stevenson-Paulik et al. 2005; Kuo et al. 2014, 2018; Land et al. 2021), DDP1 expression in plants allows for a much greater and continual accumulation of Pi over time. This increased Pi accumulation is associated with a greater induction of PSR genes in DDP1 as compared to *ipk1* seedlings (Fig. 3H). Notably, previous work on *ipk1* mutants measured PSR gene expression in roots (Kuo et al. 2014, 2018), while our work has focused on the whole plant impact of altering PP-InsPs, as above ground tissues present the greatest opportunity with regard to future phytoremediation strategies.

DDP1 and NUDIX13 functionality in planta

Overexpression of NUDIX13 in *Arabidopsis* yields similar results as overexpressing DDP1 in plants, including a reduction in PP-InsPs (Figs. 3, A to C, and 4, E to G) and an increase in Pi accumulation (Figs. 3D, 4K, and 7E). Two likely important factors for NUDIX13 to lead to these changes when overexpressed are its substrate specificity and its ability to colocalize with potential substrates.

Regarding substrate specificity, our in vitro data show the DDP1 and NUDIX13 can hydrolyze the same substrates (PP-InsPs, polyP, and Ap₅A) (Fig. 5). Our study demonstrates *Arabidopsis* NUDIX13 can hydrolyze PP-InsPs in vitro. A previous study from Olejnik et al. (2007) concluded that NUDIX13 was unable to hydrolyze InsP₇ under their reaction conditions. It is possible that this discrepancy between our results is due to our use of a more sensitive technique to quantify PP-InsP hydrolysis. It is also important to note that NUDIX13 activity on polyP had not been empirically shown in the literature before this study while other studies demonstrate DDP1 hydrolyzes polyP (Lonetti et al. 2011; Andreeva et al. 2019). We showed that overexpression of both NUDIX13 and DDP1 results in decreased PP-InsPs with a similar trend in proportionally reduced InsP₇ and InsP₈ levels (Figs. 3, A to C, and 4, E to I). Given what is known about this class of enzymes, it seems likely that both enzymes act on 1-InsP₇, 5-InsP₇, and InsP₈. However, because our measurements cannot distinguish between different isomers of PP-InsPs, we cannot say with certainty that both 1- and 5-PP-InsPs are acted on by these enzymes. It is important to note that NUDIX13 OX plants display less compromised growth as compared to DDP1 OX plants (Figs. 2, A to C, and 4, B and C), yet NUDIX13 OX leaves accumulate more Pi at a later stage of growth compared to WT plants (Fig. 4, J and K). Conversely, *nudix13-1* mutants showed increased levels of PP-InsPs and alterations in InsPs compared to WT (Supplementary Fig. S3; Table 2). These data support the role of NUDIX13 as a native plant PP-InsP phosphatase. Since there are 27 known and annotated NUDIX enzymes in *Arabidopsis* (Ogawa et al. 2008), there are likely additional NUDIX enzymes with the potential to impact Pi sensing in plants. Future studies exploring the other NUDIX enzymes will be important to expand our understanding of plant PP-InsP regulation.

Another key finding of DDP1 and NUDIX13 activity in plants stems from our localization data showing both enzymes localize to the nucleus and cytoplasm (Figs. 6 and 7D). While the specific

locations of PP-InsPs have yet to be directly determined, DDP1-GFP and NUDIX13-GFP constructs show the same localization patterns as other known InsP and PP-InsP synthetic enzymes (Xia et al. 2003; Kuo et al. 2018; Adepoju et al. 2019), which is also consistent with the native DDP1 localization in yeast (Huh et al. 2003). Interestingly, NUDIX13 was originally annotated as a mitochondrial enzyme and 1 study shows NUDIX13 is located within the mitochondria in yeast and in *Arabidopsis* suspension cells (Olejnik et al. 2007), suggesting a potentially complicated compartmentalization of NUDIX substrates across eukaryotes.

Given the ability of both DDP1 and NUDIX13 to act on other substrates, it is reasonable to ask whether the hydrolysis of these molecules is important in our plants. These alternative substrates include 2 distinct types of molecules: polyP and Ap_nAs (specifically, Ap_5A and Ap_6A), which are known substrates for DDP1 in *S. cerevisiae* (Safrany et al. 1999; Nelson et al. 2007; Lonetti et al. 2011; Márquez-Moñino et al. 2021). Both molecular classes have also been linked to maintaining Pi metabolism and cellular homeostasis in a variety of prokaryotic and eukaryotic organisms (Lorenzo-Orts et al. 2020; Pietrowska-Borek et al. 2020). Notably, polyP plays an important role in Pi sensing and storage for yeast and protozoans (Secco et al. 2012; Vila et al. 2022) and yeast polyP synthesis is controlled by PP-InsPs (Guan et al. 2023). However, there is no evidence to suggest that these other potential substrates are present in plants. Studies report careful efforts made to detect and quantify these molecules in land plants and were unsuccessful (Pietrowska-Borek et al. 2011; Zhu et al. 2019; Lorenzo-Orts et al. 2020). Given this, we hypothesize that the most likely action of DDP1 and NUDIX13 expressed in plants is to deplete the PP-InsP pool, resulting in the observed impacts on Pi accumulation and toxicity. If true, this would point to key differences between plants, yeast, and animals regarding these signaling molecules and the roles they play in vivo.

The demand for translation: from studying PP-InsPs to implementing agricultural practices

The Pi crisis is a complicated issue that will require a variety of innovative strategies to circumvent both Pi deficiency (potential shortages and Pi-deficient soils) and Pi surplus (watershed pollution and lands saturated with Pi). As the global population increases, there is a need for farmers to increase fertilizer inputs as crop production also increases. Between global food demand and higher fertilizer usage in urban areas, there is a subsequent increase in fertilizer runoff into the watersheds. One strategy that can be used is Pi phytoremediation by leveraging plants to absorb excess Pi from polluted water and soil. DDP1 overexpression in both a model species and cover crop provides unique germplasm to study how decreased PP-InsPs impact plant growth, physiology, and Pi accumulation. This study synthetically modulated PP-InsPs to increase Pi accumulation. A past study similarly targeted Pi phytoremediation through plant Pi accumulation by targeting PHR1, the transcription factor targeted by SPX1 and InsP₈, in 3 ornamental garden plant species to reclaim Pi from hydroponic solutions (Matsui et al. 2013). Matsui et al. demonstrated that overexpression of PHR1 in torenia, an ornamental plant, exhibited a leaf phenotype that was similar to DDP1 OX leaves. Another previous strategy to reduce Pi watershed pollution has targeted key genes in the InsP₆ synthesis pathway to limit InsP₆ content in seeds and grains. This strategy is important as nonruminant livestock animals cannot digest InsP₆ and so most is excreted as waste, which can pollute watersheds due to agricultural runoff (Sharpley and Withers 1994; Abelson 1999; Raboy 2002).

As we continue to learn more about the roles of PP-InsPs in plant Pi sensing and growth, this will generate knowledge for developing unique strategies, ranging from Pi removal from polluted environments to possibly improving Pi-use efficiency. Pennycress DDP1 OX transgenics are an exciting proof of concept for a Pi phytoremediation plant given the enhanced ability of DDP1-B OX transgenics to absorb Pi from soil into leaf tissue (Fig. 7). DDP1 expression in the pennycress background was effective in Pi accumulation in that working with the homozygous DDP1-B OX generation proved to be difficult based on the strong Pi toxicity symptoms (Supplementary Fig. S8). The growth tradeoff we observed when expressing DDP1 is not desirable. This was evident in our data showing that individual WT plants had the capacity to absorb significantly higher levels of P compared to DDP1 OX transgenics (Fig. 3F). However, we also note that WT plants similar in size to DDP1 OX plants accumulated significantly lower levels of P compared to DDP1 OX plants (Fig. 3G). While the current negative growth tradeoff we observe in DDP1 OX plants is undesirable, it should not be overlooked that DDP1, if expressed in a regulated fashion, could be useful for future Pi reclamation. The strategy we report here represents a step in altering PP-InsPs in planta for continual accumulation of Pi from soil, a key step for future development of unique plants to remediate Pi-polluted environments.

Materials and methods

Cloning and transformation

DDP1 (YOR163w) from *S. cerevisiae* and NUDIX13 (At3g26690) from *Arabidopsis thaliana* were PCR amplified for ligation into Gateway pENTR/D-TOPO entry vector. Using the Gateway LR Clonase II kit (Invitrogen Corp., Carlsbad, CA, USA), pENTR clones were recombined with Gateway plant destination vectors pK7FWG2 (C-terminus DDP1-GFP and NUDIX13-GFP) (VIB UGent Center for Plant Systems Biology). *Escherichia coli* transformed with these constructs was selected on antibiotic media. Plasmids purified from resulting colonies were sequenced for verification of correct cloning. *Agrobacterium tumefaciens* (strain GV3101) was transformed with these constructs and was used for transient *N. benthamiana* experiments or to transform *Arabidopsis* (ecotype Col-0) plants. All accession numbers and primer sets are available in Supplementary Table S1.

Plant growth conditions

Growth chamber

All *Arabidopsis* plants were grown on soil under long-day conditions (16-h light/8-h dark, 55% humidity, day/night temperature 23/21 °C, 120 $\mu\text{mol m}^{-2} \text{s}^{-1}$). For radiolabeling experiments, seeds were sterilized using 100% ethanol for 1 min, transferred to a 30% (v/v) Clorox solution for 5 min and washed 5 times with ddH₂O. Seeds were placed in 0.5× MS media + 0.2% agar and stratified for 3 d at 4 °C. Seedlings were transferred multiwell plates containing semisolid media (0.2% agar).

Greenhouse

Arabidopsis seeds were added to 3.2-cm square media cubes (Aeromax, Oasis Grower Solutions, Kent, OH, USA) saturated with a nutrient solution containing 230-mg/L Hydro-Gro Leafy (CropKing, Lodi, OH, USA). After 1 wk of growth, cubes were transferred into 122-cm nutrient film channels (CropKing) in a completely randomized design, comparing WT to DDP1 OX, 4 total replicates of 3 nutrient film tracks containing 18 plants fed by 1

water reservoir. Plants were initially watered with 479-mg/L Hydro-Gro Leafy at a flow rate of 0.05 mL/s, pH 6.0 ± 0.5 . After 2 wk of growth, the restriction of nutrient flow was removed, and the pump was turned off for 16 h/d (between 16:00 and 8:00).

Immunoblots of GFP-fusion proteins

Immunoblots were performed as previously reported (Burnette et al. 2003). Leaf tissue from soil-grown plants was pulverized in liquid nitrogen and proteins were separated from cell debris. SDS-bromophenol blue loading dye was added to the extracted proteins and boiled for 5 min at 85 °C. After a subsequent centrifugation, the supernatant was loaded onto a polyacrylamide gel; equal amounts of protein were added from each sample. For immunoblotting, a 1:5,000 dilution of anti-GFP antibody (Invitrogen Molecular Probes, Eugene, OR, USA) and a 1:2,000 dilution of secondary goat anti-rabbit horseradish peroxidase antibody (Bio-Rad Laboratories, Hercules, CA, USA) were used to detect GFP.

Subcellular localization and imaging

All *Arabidopsis* and *N. benthamiana* cells were imaged using a Zeiss LSM 880 confocal microscope (Carl Zeiss, Thornwood, NY, USA) equipped with a 25 \times C-Apochromat water immersion lens. *N. benthamiana* plant leaves were infiltrated with transformed with *A. tumefaciens*, as previously described (Kapila et al. 1997). Specifically, *Agrobacterium* cells were grown overnight, pelleted, and resuspended in MMA (10 mM MES, 10 mM MgCl₂, 200 μ M acetosyringone) solution at an OD₆₀₀ of 1.0. After a 2- to 4-h incubation period in the dark, *N. benthamiana* leaves were infiltrated with the *Agrobacterium* MMA cultures. Leaf sections were imaged after 24-, 48-, and 72-h postinfiltration. GFP was excited using a 488-nm argon laser and its fluorescence was detected using a 500- to 550-nm band-pass emission filter. GFP-tagged proteins were colocalized with a set of mCherry-tagged organelle markers (Nelson et al. 2007), mCherry was imaged using excitation with a HeNe 594-nm laser, and fluorescence was detected using a 600- to 650-nm band-pass emission filter. Chlorophyll autofluorescence was excited using a HeNe 594-nm laser, and emission above 650 nm was collected.

InsP and PP-InsP accumulation of *Arabidopsis* seedlings

WT and NUDIX13 OX transgenics were grown in semisolid 0.5 \times MS media and 0.2% agarose for 2 wk, 30- μ E light intensity. Twenty-four seedlings of each genotype were transferred to Eppendorf tubes containing 300 μ L of 0.5 \times MS media, 0.2% agar, and 50 μ Ci of [³H] myo-inositol (20 Ci/mmol; American Radiolabeled Chemicals [ARC], St. Louis, MO, USA) for 4 d. InsPs were extracted from seedlings by pulverizing tissue in extraction buffer (1 M perchloric acid [HClO₄], 3 mM EDTA, and 0.1 mg/mL InsP₆) and vortexed with glass beads. The pH of the extract was neutralized to pH 6 to 8 using a neutralization buffer (3 mM EDTA and 1 M K₂CO₃). Samples were dried to a volume of 80 to 100 μ L. Negatively charged species were separated via HPLC using a 125 \times 4.6 mm Partisphere SAX column (Sepax Technologies, Delaware, USA) and an ammonium phosphate elution gradient (Azevedo and Saiardi 2006). Radioactivity in all collected fractions was quantified using a scintillation counter.

Pi and P accumulation assays

Pi was extracted from ~50 mg from *Arabidopsis* and pennycress tissue of various ages. Samples were pulverized in liquid nitrogen.

A 1:10 ratio of 1% acetic acid was added to each sample, which was vortexed and incubated on ice and centrifuged. Assays were performed on Pi extracts using a modified microtiter assay as previously reported (Ames 1966). Fifty microliters of the supernatant and 1 mL of working reagent (5% w/v FeH₁₄O₁₁S \cdot 7H₂O, 1% w/v (NH₄)₂MoO₄, and 1N H₂SO₄ aq.) were incubated for an hour. Samples were placed in plastic cuvettes and absorbance at 660 nm was measured using a plate spectrophotometer. All Pi concentrations were calculated based on a standard curve from a set of standards made with known Pi concentrations. To determine total P levels, shoot mass of hydroponically-grown plants was harvested after 100 d and dried at 60 °C. Total P content was commercially analyzed at Brookside Laboratory (Bremen, OH, USA) using a nitric acid and hydrogen peroxide digestion using a MARS microwave (CEM Corporation, Mathews, NC, USA). P contents were analyzed on a 6500 Duo ICP (Thermo, Waltham, MA, USA).

RNA isolation and quantitative real-time PCR

RNA was extracted from 10-d-old seedlings grown on 0.5 \times MS media plates using a Plant RNeasy kit with on column DNase treatment (Qiagen, Germantown, MD, USA). cDNA was generated using the iScript cDNA Synthesis Kit (Bio-Rad Laboratories, Hercules, CA, USA) and 1 μ g of total RNA. Quantitative PCR was performed using ~20 ng of cDNA with PSR-specific primers and Applied Biosystems SYBR Green Universal Master Mix (Fisher Scientific, Waltham, MA, USA). All primer sequences used in the analysis can be found in Supplementary Table S1. All reactions were carried out in triplicate. Relative expression was calculated using the $\Delta\Delta$ CT method (Schmittgen and Livak 2008). Expression data were normalized to PEX4 and relative to the fold change in WT.

Expression and purification of DDP1- and NUDIX13-GST-tagged enzymes

DDP1

Gateway pENTR/D-TOPO entry vector containing DDP1 was recombined with Gateway destination vector pDEST15 (N-terminus GST; Invitrogen, Carlsbad, CA, USA) using the Gateway LR Clonase II kit (Invitrogen). After transformation of *E. coli* and selection on Carbenicillin LB plates, plasmids were purified, and sequences were verified. BL21 DE3 Turbo competent *E. coli* cells (Gelantis Biotechnology, San Diego, CA, USA) were transformed to with plasmid GST-DDP1. Single bacterial colonies expressing these constructs were picked from LB agar plates containing 50- μ g/mL carbenicillin and used to inoculate 5-mL liquid LB containing the same antibiotic concentration. This was shaken at 37 °C overnight. The following day, the culture was used as the inoculum for 250-mL LB/carb media (OD₆₀₀=0.05). The culture was shaken at 37 °C until the OD₆₀₀=0.4. Expression of DDP1 was induced with 0.1 mM IPTG (final concentration) for 4 h. Bacteria were pelleted at 5,000 \times g, for 5 min at 4 °C. The pellet was washed with 1 \times protein buffered saline (PBS), pH 7.3, centrifuged again, and stored at -80 °C.

DDP1 protein purification

A frozen pellet from 125-mL induced culture was resuspended in 6-mL lysis buffer (20 mM Tris-HCl pH 7.5, 2 mM DTT, 150 mM NaCl, 0.5% Triton X-100, 150 μ M PMSF, 300- μ L bacterial protease inhibitor [Sigma P8465], 1-mg/mL lysozyme, and 3- μ L 5- μ g/mL DNase1) for 30 min before sonicating on ice 5 times for 30 s each with 60 s in between. The lysate was centrifuged at 22,500 \times g for 20 min.

The lysate supernatant was rocked overnight at 4 °C with 0.4-mL glutathione sepharose beads (Pharmacia) that had been equilibrated with 20 mM Tris-HCl pH 7.5, 2 mM DTT, and 150 mM NaCl. The beads were collected by gentle centrifugation at 400 × *g* for 5 min. The beads were washed 3 times with 20 mM Tris-HCl pH 7.5, 2 mM DTT, and 150 mM NaCl. DDP1 was eluted from the beads with 400-μL successive elutions with 5 mM glutathione in the Tris/NaCl/DTT solution. Fraction #2 had the highest concentration of purest protein and was used for enzyme assays.

NUDIX13

Gateway pENTR/D-TOPO entry vector containing NUDIX13 was recombined with Gateway destination vector pDEST15 (Invitrogen, N-terminus GST) using the Gateway LR Clonase II kit (Invitrogen Corp., Carlsbad, CA, USA), and GST-NUDIX13 sequence was verified as above. Rosetta2 competent *E. coli* cells (Invitrogen) were transformed with plasmid GST-NUDIX13. Single bacterial colonies expressing these constructs were picked from LB agar plates containing 50-μg/mL carbenicillin and 20-μg/mL chloramphenicol. This was used to inoculate 5-mL liquid LB containing the same antibiotic concentrations and shaken at 37 °C overnight. The following day, the culture was used as the inoculum for 250-mL LB/carb/chlor media (OD₆₀₀ = 0.05). The culture was shaken at 37 °C until the OD₆₀₀ = 0.7. Expression of DDP1 was induced with 1 mM IPTG (final concentration) for 3 h. Bacteria were pelleted at 5,000 × *g*, for 5 min at 4 °C. The pellet was washed with 1× PBS, pH 7.3, centrifuged again, and stored at –80 °C.

NUDIX13 protein purification

A frozen pellet from 125-mL induced culture was resuspended in 6-mL lysis buffer (1× PBS, pH 7.3, 1 mM DTT, 0.5% Triton X-100, 150 μM PMSF, 1-mg/mL lysozyme, and 3-μL 5-μg/mL DNase1) for 30 min before sonicating on ice 5 times for 30 s each with 60 s in between. The lysate was centrifuged at 22,500 × *g* for 20 min. The lysate supernatant was rocked overnight at 4 °C with 0.4-mL glutathione sepharose beads (Pharmacia) that had been equilibrated with 1× PBS, pH 7.3, 1 mM DTT, and 0.5% Triton X-100. The beads were collected by gentle centrifugation at 400 × *g* for 5 min. The beads were washed 3 times with 50 mM Tris-HCl pH 8.0, 350 mM NaCl, and 1 mM DTT. NUDIX13 was eluted from the beads with 400-μL successive elutions with 5 mM glutathione in the Tris/NaCl/DTT solution. Fraction #2 had the highest concentration of purest protein and was used for enzyme assays.

Ap₄A and polyP hydrolysis enzyme assays

Ap₄A (D4022), Ap₅A (D1262), and polyP were purchased from Sigma. Fifty-microliter reactions containing 14-μg purified NUDIX13-GST were incubated with 1 mM DTT, 100 mM Tris-HCl (pH 8.5), 5 mM MgCl₂, and 0.68 mM Ap₄A/Ap₅A or 50-μg polyP (Olejnik et al. 2007). These conditions were the same for DDP1-GST hydrolysis assays except 50 mM HEPES (pH 7.0) and 50 mM KCl were used instead of Tris-HCl (modified from Lonetti et al. 2011). All reactions were incubated at 37 °C for 30 min and chemically inactivated using 0.25 M EDTA and placed on ice. Once terminated, 5 μL of 6XOrangeG dye was added to each sample. Samples were loaded onto phytate gels (35.5% acrylamide and 10× TBE) (Losito et al. 2009). Phytate gels were run overnight at 400 V, stained using toluidine blue staining solution (0.05% toluidine blue, 20% methanol, 2% glycerol, and 20 mM Tris-HCl pH 6.8 to 7.0) for 2 min, and destained with H₂O for 30 s to 5 min.

PP-InsP hydrolysis enzyme assays

Substrates for PP-InsP hydrolysis enzyme assays were synthesized using the in vitro substrate synthesis system from commercially available [³H] Ins(1,4,5)P₃ (17.1 Ci/mmol; ARC, St. Louis, MO, USA) and purified enzymes as described in Adepoju et al. (2019). Enzyme activity assays were performed according to Olejnik et al. (2007) with the following modification: DDP1, NUDIX13, and GST assays were performed in a 50-μL reaction at 37 °C for 30 min using 40 μg of purified enzyme.

Accession numbers

Sequence data and accession numbers from this article can be found in [Supplementary Table S1](#).

Acknowledgments

We gratefully thank Dr. John Sedbrook and Dr. Maliheh Esfahanian for the advice on pennycress and transformation protocols.

Author contributions

C.F. and G.G. conceived this project; C.F., B.C., S.P.W., J.O., and G.G. designed the experiments. C.F. and B.C. performed subcellular imaging and seedling PP-InsP levels. C.F., C.P., and J.K. phenotyped the plants. C.F., C.P., C.C., and J.K. performed the phosphate assays. H.B. and J.O. designed and performed the greenhouse experiments. C.F., B.C., and J.D. performed the enzyme assays. C.F., B.C., J.D., C.C., J.O., and G.G. analyzed and interpreted the data. C.F. wrote the manuscript and prepared the figures.

Supplementary data

The following materials are available in the online version of this article.

Supplementary Figure S1. Additional InsP and PP-InsP profiles of DDP1 OX transgenics.

Supplementary Figure S2. Additional InsP and PP-InsP profiles of NUDIX13 OX transgenics.

Supplementary Figure S3. InsP and PP-InsP profiles of *nudix13-1* plants.

Supplementary Figure S4. DDP1-GFP and NUDIX13-GFP localization in *Arabidopsis* epidermal cells.

Supplementary Figure S5. Transient DDP1-GFP expression after 24 and 48 h.

Supplementary Figure S6. Transient NUDIX13-GFP expression in *N. benthamiana* leaves 24- and 48-h postinfiltration.

Supplementary Figure S7. *N. benthamiana* leaves co-infiltrated with YFP-DDP1, unconjugated mCherry, and ER-mCherry.

Supplementary Figure S8. Homozygous pennycress DDP1-B OX plants.

Supplementary Table S1. Oligonucleotides used in this study.

Funding

This work was funded in part by the USDA National Institute of Food and Agriculture (AFRI Postdoctoral Fellowship 1031638), Hatch project VA-136334, the National Science Foundation to G.G. (MCB 1616038), and through the Virginia Tech Institute for Critical Technologies and Applied Science and Applied Sciences (ICALS).

Conflict of interest statement. G.G. and C.F. have patents pending for the use of DDP1 and NUDIX13 in plants. The remaining authors have no conflict of interest to declare.

Data availability

The data underlying this article are available in the article and in its online supplementary material.

References

- Abelson PH. A potential phosphate crisis. *Science*. 1999;283(5410):2015–2015. <https://doi.org/10.1126/science.283.5410.2015>
- Aceti DJ, Bitto E, Yakunin AF, Proudfoot M, Bingman CA, Frederick RO, Sreenath HK, Vojtik FC, Wrobel RL, Fox BG, et al. Structural and functional characterization of a novel phosphatase from the *Arabidopsis thaliana* gene locus At1g05000. *Proteins*. 2008;73(1):241–253. <https://doi.org/10.1002/prot.22041>
- Adepoju O, Williams SP, Craig B, Cridland CA, Sharpe AK, Brown AM, Land E, Perera IY, Mena D, Sobrado P, et al. Inositol trisphosphate kinase and diphosphoinositol pentakisphosphate kinase enzymes constitute the inositol pyrophosphate synthesis pathway in plants. *bioRxiv*. <https://doi.org/10.1101/724914>, 2019, preprint: not peer reviewed.
- Alford SR, Rangarajan P, Williams P, Gillaspay GE. *myo*-Inositol oxygenase is required for responses to low energy conditions in *Arabidopsis thaliana*. *Front Plant Sci*. 2012;3:69. <https://doi.org/10.3389/fpls.2012.00069>
- Altschul SF, Madden TL, Schäffer AA, Zhang J, Zhang Z, Miller W, Lipman DJ. Gapped BLAST and PSI-BLAST: a new generation of protein database search programs. *Nucleic Acids Res*. 1997;25(17):3389–3402. <https://doi.org/10.1093/nar/25.17.3389>
- Altschul SF, Wootton JC, Gertz EM, Agarwala R, Morgulis A, Schäffer AA, Yu Y-K. Protein database searches using compositionally adjusted substitution matrices. *FEBS J*. 2005;272(20):5101–5109. <https://doi.org/10.1111/j.1742-4658.2005.04945.x>
- Ames BN. [10] Assay of inorganic phosphate, total phosphate and phosphatases. *Methods in enzymology*. Academic Press; 1966. p. 115–118. <https://www.sciencedirect.com/science/article/pii/0076687966080145>
- Andreeva N, Ledova L, Ryazanova L, Tomashevsky A, Kulakovskaya T, Eldarov M. Ppn2 endopolyphosphatase overexpressed in *Saccharomyces cerevisiae*: comparison with Ppn1, Ppx1, and Ddp1 polyphosphatases. *Biochimie*. 2019;163:101–107. <https://doi.org/10.1016/j.biochi.2019.06.001>
- Aung K, Lin S-I, Wu C-C, Huang Y-T, Su C, Chiou T-J. Pho2, a phosphate overaccumulator, is caused by a nonsense mutation in a microRNA399 target gene. *Plant Physiol*. 2006;141(3):1000–1011. <https://doi.org/10.1104/pp.106.078063>
- Azevedo C, Saiardi A. Extraction and analysis of soluble inositol polyphosphates from yeast. *Nat Protoc*. 2006;1(5):2416–2422. <https://doi.org/10.1038/nprot.2006.337>
- Azevedo C, Saiardi A. Eukaryotic phosphate homeostasis: the inositol pyrophosphate perspective. *Trends Biochem Sci*. 2017;42(3):219–231. <https://doi.org/10.1016/j.tibs.2016.10.008>
- Bari R, Datt Pant B, Stitt M, Scheible W-R. PHO2, MicroRNA399, and PHR1 define a phosphate-signaling pathway in plants. *Plant Physiol*. 2006;141(3):988–999. <https://doi.org/10.1104/pp.106.079707>
- Burnette RN, Gunesequera BM, Gillaspay GE. An *Arabidopsis* inositol 5-phosphatase gain-of-function alters abscisic acid signaling. *Plant Physiol*. 2003;132(2):1011–1019. <https://doi.org/10.1104/pp.019000>
- Cartwright JL, McLennan AG. The *Saccharomyces cerevisiae* YOR163w gene encodes a diadenosine 5',5''-P₁,P₆-hexaphosphate (Ap6A) hydrolase member of the MutT motif (Nudix hydrolase) family. *J Biol Chem*. 1999;274(13):8604–8610. <https://doi.org/10.1074/jbc.274.13.8604>
- Chien P-S, Chiang C-P, Leong SJ, Chiou T-J. Sensing and signaling of phosphate starvation: from local to long distance. *Plant Cell Physiol*. 2018;59(9):1714–1722. <https://doi.org/10.1093/pcp/pcy148>
- Cho H, Bouain N, Zheng L, Rouached H. Plant resilience to phosphate limitation: current knowledge and future challenges. *Crit Rev Biotechnol*. 2021;41(1):63–71. <https://doi.org/10.1080/07388551.2020.1825321>
- Chopra R, Johnson EB, Emenecker R, Cahoon EB, Lyons J, Kliebenstein DJ, Daniels E, Dorn KM, Esfahanian M, Folstad N, et al. Identification and stacking of crucial traits required for the domestication of pennycress. *Nat Food*. 2020;1(1):84–91. <https://doi.org/10.1038/s43016-019-0007-z>
- Cordell D, Drangert J-O, White S. The story of phosphorus: global food security and food for thought. *Glob Environ Change*. 2009;19(2):292–305. <https://doi.org/10.1016/j.gloenvcha.2008.10.009>
- Cordell D, White S. Peak phosphorus: clarifying the key issues of a vigorous debate about long-term phosphorus security. *Sustainability*. 2011;3(10):2027–2049. <https://doi.org/10.3390/su3102027>
- Desai M, Rangarajan P, Donahue JL, Williams SP, Land ES, Mandal MK, Phillippy BQ, Perera IY, Raboy V, Gillaspay GE. Two inositol hexakisphosphate kinases drive inositol pyrophosphate synthesis in plants. *Plant J*. 2014;80(4):642–653. <https://doi.org/10.1111/tbj.12669>
- Dollins DE, Bai W, Fridy PC, Otto JC, Neubauer JL, Gattis SG, Mehta KPM, York JD. Vip1 is a kinase and pyrophosphatase switch that regulates inositol diphosphate signaling. *Proc Natl Acad Sci U S A*. 2020;117(17):9356–9364. <https://doi.org/10.1073/pnas.1908875117>
- Dong J, Ma G, Sui L, Wei M, Satheesh V, Zhang R, Ge S, Li J, Zhang T-E, Wittwer C, et al. Inositol pyrophosphate InsP₈ acts as an intracellular phosphate signal in *Arabidopsis*. *Mol Plant*. 2019;12(11):1463–1473. <https://doi.org/10.1016/j.molp.2019.08.002>
- Gaugler P, Schneider R, Liu G, Qiu D, Weber J, Schmid J, Jork N, Häner M, Ritter K, Fernández-Rebollo N, et al. *Arabidopsis* PFA-DSP-type phosphohydrolases target specific inositol pyrophosphate messengers. *Biochemistry*. 2022;61(12):1213–1227. <https://doi.org/10.1021/acs.biochem.2c00145>
- Gobler CJ. Climate change and harmful algal blooms: insights and perspective. *Harmful Algae*. 2020;91:101731. <https://doi.org/10.1016/j.hal.2019.101731>
- Guan Z, Chen J, Liu R, Chen Y, Xing Q, Du Z, Cheng M, Hu J, Zhang W, Mei W, et al. The cytoplasmic synthesis and coupled membrane translocation of eukaryotic polyphosphate by signal-activated VTC complex. *Nat Commun*. 2023;14(1):718. <https://doi.org/10.1038/s41467-023-36466-4>
- Guan Z, Zhang Q, Zhang Z, Zuo J, Chen J, Liu R, Savarin J, Broger L, Cheng P, Wang Q, et al. Mechanistic insights into the regulation of plant phosphate homeostasis by the rice SPX2-PHR2 complex. *Nat Commun*. 2022;13(1):1581. <https://doi.org/10.1038/s41467-022-29275-8>
- Gunawardana D, Likic VA, Gayler KR. A comprehensive bioinformatics analysis of the Nudix superfamily in *Arabidopsis thaliana*. *Comp Funct Genomics*. 2009;2009:820381. <https://doi.org/10.1155/2009/820381>
- Hu B, Zhu C, Li F, Tang J, Wang Y, Lin A, Liu L, Che R, Chu C. LEAF TIP NECROSIS1 plays a pivotal role in the regulation of multiple phosphate starvation responses in rice. *Plant Physiol*. 2011;156(3):1101–1115. <https://doi.org/10.1104/pp.110.170209>

- Huh W-K, Falvo JV, Gerke LC, Carroll AS, Howson RW, Weissman JS, O'Shea EK. Global analysis of protein localization in budding yeast. *Nature*. 2003;425(6959):686–691. <https://doi.org/10.1038/nature02026>
- Irvine RF, Schell MJ. Back in the water: the return of the inositol phosphates. *Nat Rev Mol Cell Biol*. 2001;2(5):327–338. <https://doi.org/10.1038/35073015>
- Jost R, Pharmawati M, Lapis-Gaza HR, Rossig C, Berkowitz O, Lambers H, Finnegan PM. Differentiating phosphate-dependent and phosphate-independent systemic phosphate-starvation response networks in *Arabidopsis thaliana* through the application of phosphite. *J Exp Bot*. 2015;66(9):2501–2514. <https://doi.org/10.1093/jxb/erv025>
- Kapila J, De Rycke R, Van Montagu M, Angenon G. An *Agrobacterium*-mediated transient gene expression system for intact leaves. *Plant Sci*. 1997;122(1):101–108. [https://doi.org/10.1016/S0168-9452\(96\)04541-4](https://doi.org/10.1016/S0168-9452(96)04541-4)
- Kilari RS, Weaver JD, Shears SB, Safrany ST. Understanding inositol pyrophosphate metabolism and function: kinetic characterization of the DIPPs. *FEBS Lett*. 2013;587(21):3464–3470. <https://doi.org/10.1016/j.febslet.2013.08.035>
- Kraszewska E. The plant Nudix hydrolase family. *Acta Biochim Pol*. 2008;55(4):663–671. https://doi.org/10.18388/abp.2008_3025
- Kuo H, Chang T, Chiang S, Wang W, Charng Y, Chiou T. *Arabidopsis* inositol pentakisphosphate 2-kinase, AtIPK1, is required for growth and modulates phosphate homeostasis at the transcriptional level. *Plant J*. 2014;80(3):503–515. <https://doi.org/10.1111/tpj.12650>
- Kuo H-F, Hsu Y-Y, Lin W-C, Chen K-Y, Munnik T, Brearley CA, Chiou T-J. *Arabidopsis* inositol phosphate kinases IPK1 and ITPK1 constitute a metabolic pathway in maintaining phosphate homeostasis. *Plant J*. 2018;95(4):613–630. <https://doi.org/10.1111/tpj.13974>
- Laha D, Johnen P, Azevedo C, Dynowski M, Weiß M, Capolicchio S, Mao H, Iven T, Steenbergen M, Freyer M, et al. VIH2 regulates the synthesis of inositol pyrophosphate InsP₈ and jasmonate-dependent defenses in *Arabidopsis*. *Plant Cell*. 2015;27(4):1082–1097. <https://doi.org/10.1105/tpc.114.135160>
- Laha D, Parvin N, Dynowski M, Johnen P, Mao H, Bitters ST, Zheng N, Schaaf G. Inositol polyphosphate binding specificity of the jasmonate receptor complex1. *Plant Physiol*. 2016;171(4):2364–2370. <https://doi.org/10.1104/pp.16.00694>
- Laha D, Parvin N, Hofer A, Giehl RFH, Fernandez-Rebollo N, von Wirén N, Saiardi A, Jessen HJ, Schaaf G. *Arabidopsis* ITPK1 and ITPK2 have an evolutionarily conserved phytic acid kinase activity. *ACS Chem Biol*. 2019;14(10):2127–2133. <https://doi.org/10.1021/acscchembio.9b00423>
- Laha D, Portela-Torres P, Desfougères Y, Saiardi A. Inositol phosphate kinases in the eukaryote landscape. *Adv Biol Regul*. 2021;79:100782. <https://doi.org/10.1016/j.jbior.2020.100782>
- Laha NP, Giehl RFH, Riemer E, Qiu D, Pullagurla NJ, Schneider R, Dhir YW, Yadav R, Mihiret YE, Gaugler P, et al. INOSITOL (1,3,4) TRIPHOSPHATE 5/6 KINASE1-dependent inositol polyphosphates regulate auxin responses in *Arabidopsis*. *Plant Physiol*. 2022;190(4):2722–2738. <https://doi.org/10.1093/plphys/kiac425>
- Land ES, Cridland CA, Craigie B, Dye A, Hildreth SB, Helm RF, Gillaspay GE, Perera IY. A role for inositol pyrophosphates in the metabolic adaptations to low phosphate in *Arabidopsis*. *Metabolites*. 2021;11(9):601. <https://doi.org/10.3390/metabo11090601>
- Liu J, Guan Z, Liu H, Qi L, Zhang D, Zou T, Yin P. Structural insights into the substrate recognition mechanism of *Arabidopsis* GPP-bound NUDX1 for noncanonical monoterpene biosynthesis. *Mol Plant*. 2018;11(1):218–221. <https://doi.org/10.1016/j.molp.2017.10.006>
- Liu T-Y, Aung K, Tseng C-Y, Chang T-Y, Chen Y-S, Chiou T-J. Vacuolar Ca²⁺/H⁺ transport activity is required for systemic phosphate homeostasis involving shoot-to-root signaling in *Arabidopsis*. *Plant Physiol*. 2011;156(3):1176–1189. <https://doi.org/10.1104/pp.111.175257>
- Livermore TM, Azevedo C, Kolozsvari B, Wilson MSC, Saiardi A. Phosphate, inositol and polyphosphates. *Biochem Soc Trans*. 2016;44(1):253–259. <https://doi.org/10.1042/BST20150215>
- Lonetti A, Szigyarto Z, Bosch D, Loss O, Azevedo C, Saiardi A. Identification of an evolutionarily conserved family of inorganic polyphosphate endopolyphosphatases. *J Biol Chem*. 2011;286(37):31966–31974. <https://doi.org/10.1074/jbc.M111.266320>
- Lorenzo-Orts L, Couto D, Hothorn M. Identity and functions of inorganic and inositol polyphosphates in plants. *New Phytol*. 2020;225(2):637–652. <https://doi.org/10.1111/nph.16129>
- Losito O, Szigyarto Z, Resnick AC, Saiardi A. Inositol pyrophosphates and their unique metabolic complexity: analysis by gel electrophoresis. *PLoS One*. 2009;4(5):e5580. <https://doi.org/10.1371/journal.pone.0005580>
- Madison I, Gillan L, Peace J, Gabrieli F, Van den Broeck L, Jones JL, Sozzani R. Phosphate starvation: response mechanisms and solutions. *J Exp Bot*. 2023;74(21):6417–6430. <https://doi.org/10.1093/jxb/erad326>
- Márquez-Moñino MÁ, Ortega-García R, Shipton ML, Franco-Echevarría E, Riley AM, Sanz-Aparicio J, Potter BVL, González B. Multiple substrate recognition by yeast diadenosine and diphosphoinositol polyphosphate phosphohydrolase through phosphate clamping. *Sci Adv*. 2021;7(17):eabf6744. <https://doi.org/10.1126/sciadv.abf6744>
- Martín AC, del Pozo JC, Iglesias J, Rubio V, Solano R, de La Peña A, Leyva A, Paz-Ares J. Influence of cytokinins on the expression of phosphate starvation responsive genes in *Arabidopsis*. *Plant J*. 2000;24(5):559–567. <https://doi.org/10.1046/j.1365-313x.2000.00893.x>
- Matsui K, Togami J, Mason JG, Chandler SF, Tanaka Y. Enhancement of phosphate absorption by garden plants by genetic engineering: a new tool for phytoremediation. *BioMed Res Int*. 2013;7:182032. <https://doi.org/10.1155/2013/182032>
- McCormick S. Ta Ta for now: *Thlapsi arvensis* (pennycress), an emerging model for genetic analyses. *Plant J*. 2018;96(6):1091–1092. <https://doi.org/10.1111/tpj.14172>
- Menezes-Blackburn D, Giles C, Darch T, George TS, Blackwell M, Stutter M, Shand C, Lumsdon D, Cooper P, Wendler R, et al. Opportunities for mobilizing recalcitrant phosphorus from agricultural soils: a review. *Plant Soil*. 2018;427(1–2):5–16. <https://doi.org/10.1007/s11104-017-3362-2>
- Morrisette VA, Rolfs RJ. The intersection between stress responses and inositol pyrophosphates in *Saccharomyces cerevisiae*. *Curr Genet*. 2020;66(5):901–910. <https://doi.org/10.1007/s00294-020-01078-8>
- Mulugu S, Bai W, Fridy PC, Bastidas RJ, Otto JC, Dollins DE, Haystead TA, Ribeiro AA, York JD. A conserved family of enzymes that phosphorylate inositol hexakisphosphate. *Science*. 2007;316(5821):106–109. <https://doi.org/10.1126/science.1139099>
- Nagarajan VK, Jain A, Poling MD, Lewis AJ, Raghothama KG, Smith AP. *Arabidopsis* Pht1;5 mobilizes phosphate between source and sink organs and influences the interaction between phosphate homeostasis and ethylene signaling. *Plant Physiol*. 2011;156(3):1149–1163. <https://doi.org/10.1104/pp.111.174805>
- Nelson BK, Cai X, Nebenführ A. A multicolored set of in vivo organelle markers for co-localization studies in *Arabidopsis* and other plants. *Plant J*. 2007;51(6):1126–1136. <https://doi.org/10.1111/j.1365-313X.2007.03212.x>

- Ogawa T, Yoshimura K, Miyake H, Ishikawa K, Ito D, Tanabe N, Shigeoka S. Molecular characterization of organelle-type Nudix hydrolases in *Arabidopsis*. *Plant Physiol.* 2008;148(3):1412–1424. <https://doi.org/10.1104/pp.108.128413>
- Olejnik K, Murcha MW, Whelan J, Kraszewska E. Cloning and characterization of AtNUDT13, a novel mitochondrial *Arabidopsis thaliana* Nudix hydrolase specific for long-chain diadenosine polyphosphates. *FEBS J.* 2007;274(18):4877–4885. <https://doi.org/10.1111/j.1742-4658.2007.06009.x>
- Pietrowska-Borek M, Dobrogojski J, Sobieszczuk-Nowicka E, Borek S. New insight into plant signaling: extracellular ATP and uncommon nucleotides. *Cells.* 2020;9(2):345. <https://doi.org/10.3390/cells9020345>
- Pietrowska-Borek M, Nuc K, Zielezińska M, Guranowski A. Diadenosine polyphosphates (Ap3A and Ap4A) behave as alarmones triggering the synthesis of enzymes of the phenylpropanoid pathway in *Arabidopsis thaliana*. *FEBS Open Bio.* 2011;1(1):1–6. <https://doi.org/10.1016/j.fob.2011.10.002>
- Puga MI, Mateos I, Charukesi R, Wang Z, Franco-Zorrilla JM, de Lorenzo L, Irigoyen ML, Masiero S, Bustos R, Rodríguez J, et al. SPX1 is a phosphate-dependent inhibitor of phosphate starvation response 1 in *Arabidopsis*. *Proc Natl Acad Sci U S A.* 2014;111(41):14947–14952. <https://doi.org/10.1073/pnas.1404654111>
- Raboy V. Progress in breeding low phytate crops. *J Nutr.* 2002;132(3):503S–505S. <https://doi.org/10.1093/jn/132.3.503S>
- Raboy V, Young KA, Dorsch JA, Cook A. Genetics and breeding of seed phosphorus and phytic acid. *J Plant Physiol.* 2001;158(4):489–497. <https://doi.org/10.1078/0176-1617-00361>
- Ried MK, Wild R, Zhu J, Pipercevic J, Sturm K, Broger L, Harmel RK, Abriata LA, Hothorn LA, Fiedler D, et al. Inositol pyrophosphates promote the interaction of SPX domains with the coiled-coil motif of PHR transcription factors to regulate plant phosphate homeostasis. *Nat Commun.* 2021;12(1):384. <https://doi.org/10.1038/s41467-020-20681-4>
- Riemer E, Qiu D, Laha D, Harmel RK, Gaugler P, Gaugler V, Frei M, Hajirezaei M-R, Laha NP, Krusenbaum L, et al. ITPK1 is an InsP₆/ADP phosphotransferase that controls phosphate signaling in *Arabidopsis*. *Mol Plant.* 2021;14(11):1864–1880. <https://doi.org/10.1016/j.molp.2021.07.011>
- Rouached H, Arpat AB, Poirier Y. Regulation of phosphate starvation responses in plants: signaling players and cross-talks. *Mol Plant.* 2010;3(2):288–299. <https://doi.org/10.1093/mp/ssp120>
- Safrany ST, Ingram SW, Cartwright JL, Falck JR, McLennan AG, Barnes LD, Shears SB. The diadenosine hexaphosphate hydrolases from *Schizosaccharomyces pombe* and *Saccharomyces cerevisiae* are homologues of the human diphosphoinositol polyphosphate phosphohydrolase: overlapping substrate specificities in a mutant-type protein. *J Biol Chem.* 1999;274(31):21735–21740. <https://doi.org/10.1074/jbc.274.31.21735>
- Schmittgen TD, Livak KJ. Analyzing real-time PCR data by the comparative C(T) method. *Nat Protoc.* 2008;3(6):1101–1108. <https://doi.org/10.1038/nprot.2008.73>
- Secco D, Wang C, Shou H, Whelan J. Phosphate homeostasis in the yeast *Saccharomyces cerevisiae*, the key role of the SPX domain-containing proteins. *FEBS Lett.* 2012;586(4):289–295. <https://doi.org/10.1016/j.febslet.2012.01.036>
- Sharpley AN, Withers PJA. The environmentally-sound management of agricultural phosphorus. *Fertilizer Research.* 1994;39(2):133–146. <https://doi.org/10.1007/BF00750912>
- Sheard LB, Tan X, Mao H, Withers J, Ben-Nissan G, Hinds TR, Kobayashi Y, Hsu F-F, Sharon M, Browse J, et al. Jasmonate perception by inositol phosphate-potentiated COI1-JAZ co-receptor. *Nature.* 2010;468(7322):400–405. <https://doi.org/10.1038/nature09430>
- Shears SB. Inositol pyrophosphates: why so many phosphates? *Adv Biol Regul.* 2015;57:203–216. <https://doi.org/10.1016/j.jbior.2014.09.015>
- Shears SB. Intimate connections: inositol pyrophosphates at the interface of metabolic regulation and cell signaling. *J Cell Physiol.* 2018;233(3):1897–1912. <https://doi.org/10.1002/jcp.26017>
- Shears SB, Baughman BM, Gu C, Nair VS, Wang H. The significance of the 1-kinase/1-phosphatase activities of the PPIP5K family. *Adv Biol Regul.* 2017;63:98–106. <https://doi.org/10.1016/j.jbior.2016.10.003>
- Sheikh S, O’Handley SF, Dunn CA, Bessman MJ. Identification and characterization of the Nudix hydrolase from the Archaeon, *Methanococcus jannaschii*, as a highly specific ADP-ribose pyrophosphatase. *J Biol Chem.* 1998;273(33):20924–20928. <https://doi.org/10.1074/jbc.273.33.20924>
- Srouji JR, Xu A, Park A, Kirsch JF, Brenner SE. The evolution of function within the Nudix homology clan. *Proteins.* 2017;85(5):775–811. <https://doi.org/10.1002/prot.25223>
- Stefanovic A, Ribot C, Rouached H, Wang Y, Chong J, Belbahri L, Delessert S, Poirier Y. Members of the PHO1 gene family show limited functional redundancy in phosphate transfer to the shoot, and are regulated by phosphate deficiency via distinct pathways. *Plant J.* 2007;50(6):982–994. <https://doi.org/10.1111/j.1365-3113.2007.03108.x>
- Stevenson-Paulik J, Bastidas RJ, Chiou S-T, Frye RA, York JD. Generation of phytate-free seeds in *Arabidopsis* through disruption of inositol polyphosphate kinases. *Proc Natl Acad Sci U S A.* 2005;102(35):12612–12617. <https://doi.org/10.1073/pnas.0504172102>
- Tan X, Calderon-Villalobos LIA, Sharon M, Zheng C, Robinson CV, Estelle M, Zheng N. Mechanism of auxin perception by the TIR1 ubiquitin ligase. *Nature.* 2007;446(7136):640–645. <https://doi.org/10.1038/nature05731>
- Tang Q, Liu C, Zhong C, Ding J. Crystal structures of *Arabidopsis thaliana* nudix hydrolase NUDT7 reveal a previously unobserved conformation. *Mol Plant.* 2015;8(10):1557–1559. <https://doi.org/10.1016/j.molp.2015.07.010>
- Thota SG, Bhandari R. The emerging roles of inositol pyrophosphates in eukaryotic cell physiology. *J Biosci.* 2015;40(3):593–605. <https://doi.org/10.1007/s12038-015-9549-x>
- Tsui MM, York JD. Roles of inositol phosphates and inositol pyrophosphates in development, cell signaling and nuclear processes. *Adv Enzyme Regul.* 2010;50(1):324–337. <https://doi.org/10.1016/j.advenzreg.2009.12.002>
- Vaccari DA. Phosphorus: a looming crisis. *Sci Am.* 2009;300(6):54–59. <https://doi.org/10.1038/scientificamerican0609-54>
- Vance CP, Uhde-Stone C, Allan DL. Phosphorus acquisition and use: critical adaptations by plants for securing a nonrenewable resource. *New Phytol.* 2003;157(3):423–447. <https://doi.org/10.1046/j.1469-8137.2003.00695.x>
- Vila T, Frases S, Gomes FM. Lessons from protozoans: phosphate sensing and polyphosphate storage in fungi. *PLoS Pathog.* 2022;18(3):e1010298. <https://doi.org/10.1371/journal.ppat.1010298>
- Wang H, Gu C, Rolfes RJ, Jessen HJ, Shears SB. Structural and biochemical characterization of Siw14: a protein-tyrosine phosphatase fold that metabolizes inositol pyrophosphates. *J Biol Chem.* 2018;293(18):6905–6914. <https://doi.org/10.1074/jbc.RA117.001670>
- Wang Z, Kuo H-F, Chiou T-J. Intracellular phosphate sensing and regulation of phosphate transport systems in plants. *Plant Physiol.* 2021;187(4):2043–2055. <https://doi.org/10.1093/plphys/kiab343>

- Whitfield H, White G, Sprigg C, Riley AM, Potter BVL, Hemmings AM, Brearley CA. An ATP-responsive metabolic cassette comprised of inositol tris/tetrakisphosphate kinase 1 (ITPK1) and inositol pentakisphosphate 2-kinase (IPK1) buffers diphosphoinositol phosphate levels. *Biochem J.* 2020;477(14):2621–2638. <https://doi.org/10.1042/BCJ20200423>
- Wild R, Gerasimaite R, Jung J-Y, Truffault V, Pavlovic I, Schmidt A, Saiardi A, Jessen HJ, Poirier Y, Hothorn M, et al. Control of eukaryotic phosphate homeostasis by inositol polyphosphate sensor domains. *Science.* 2016;352(6288):986–990. <https://doi.org/10.1126/science.aad9858>
- Williams SP, Gillaspay GE, Perera IY. Biosynthesis and possible functions of inositol pyrophosphates in plants. *Front Plant Sci.* 2015;6:67. <https://doi.org/10.3389/fpls.2015.00067>
- Xia H-J, Brearley C, Elge S, Kaplan B, Fromm H, Mueller-Roeber B. *Arabidopsis* inositol polyphosphate 6-/3-kinase is a nuclear protein that complements a yeast mutant lacking a functional ArgR-Mcm1 transcription complex. *Plant Cell.* 2003;15(2):449–463. <https://doi.org/10.1105/tpc.006676>
- Xu W, Gauss P, Shen J, Dunn CA, Bessman MJ. The gene *e.1* (*nudE.1*) of T4 bacteriophage designates a new member of the Nudix hydrolase superfamily active on flavin adenine dinucleotide, adenosine 5'-triphospho-5'-adenosine, and ADP-ribose. *J Biol Chem.* 2002;277(26):23181–23185. <https://doi.org/10.1074/jbc.M203325200>
- Zhou J, Hu Q, Xiao X, Yao D, Ge S, Ye J, Li H, Cai R, Liu R, Meng F, et al. Mechanism of phosphate sensing and signaling revealed by rice SPX1-PHR2 complex structure. *Nat Commun.* 2021;12(1):7040. <https://doi.org/10.1038/s41467-021-27391-5>
- Zhu J, Lau K, Puschmann R, Harmel RK, Zhang Y, Pries V, Gaugler P, Broger L, Dutta AK, Jessen HJ, et al. Two bifunctional inositol pyrophosphate kinases/phosphatases control plant phosphate homeostasis. *eLife.* 2019;8:e43582. <https://doi.org/10.7554/eLife.43582>